

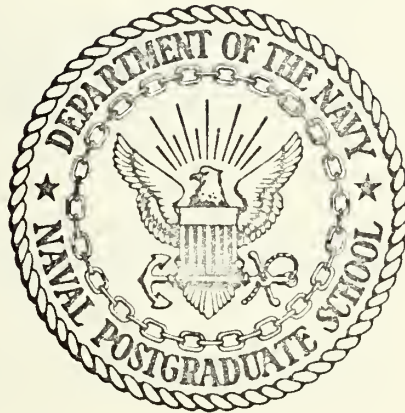
COMPUTER SIMULATION OF SPLIT INTERSTITIAL
EQUILIBRIUM POSITIONS AND BINDING ENER-
GIES IN A TUNGSTEN CRYSTAL

James Anthony Tankovich

DUDLEY KNOX LIBRARY
NAVAL POSTGRADUATE SCHOOL
MONTEREY, CALIFORNIA 93943-5002

NAVAL POSTGRADUATE SCHOOL

Monterey, California



THESIS

COMPUTER SIMULATION OF SPLIT INTERSTITIAL
EQUILIBRIUM POSITIONS AND BINDING ENERGIES
IN A TUNGSTEN CRYSTAL

by

James Anthony Tankovich

Thesis Advisor:

D.E. Harrison, Jr.

June 1972

Approved for public release; distribution unlimited.

Computer Simulation of Split Interstitial
Equilibrium Positions and Binding Energies
in a Tungsten Crystal

by

James Anthony Tankovich
Captain, United States Army
B.S., United States Military Academy, 1967

Submitted in partial fulfillment of the
requirements for the degree of

MASTER OF SCIENCE IN PHYSICS

from the

NAVAL POSTGRADUATE SCHOOL
June 1972

ABSTRACT

Computer simulations were performed to locate the equilibrium positions and binding energies of interstitial He, Ne, Ar, Kr, and Xe atoms in a tungsten crystal. Heavy interstitial atoms in tungsten share a lattice site with the atom that normally occupies that site and form what is called a split interstitial. Three characteristic interstitial sites were located relative to each lattice site tested. The distance of the impurity atom from the site was seen to vary roughly inversely with its mass, and the displacement of the lattice atom increased with the mass of the impurity atom.

The foreign atom in its interstitial position was tested to determine the minimum initial kinetic energy needed to escape the lattice, as well as the optimum escape direction. The minimum energy may be interpreted to be the binding energy of the defect. A comparison of experimental binding energies from Kornelsen and Sinha and simulated binding energies indicates the model gives realistic results.

TABLE OF CONTENTS

I.	INTRODUCTION-----	8
II.	NATURE OF THE PROBLEM-----	9
	A. HISTORICAL BACKGROUND-----	9
	B. CHOICE OF POTENTIAL FUNCTION-----	12
	C. EXPERIMENTAL RESULTS OF KORNELSEN AND SINHA----	14
III.	SIMULATION MODEL-----	15
	A. THE CRYSTAL-----	15
	B. THE TIMESTEP INTERVAL-----	16
IV.	SIMULATION PROCEDURE-----	18
	A. STATIC SIMULATION-----	18
	B. DYNAMIC SIMULATION-----	20
V.	PRESENTATION OF DATA-----	22
	A. STATIC RUNS-----	22
	1. Preliminary Testing of the Static Program --	22
	2. Positions for Helium in Tungsten-----	23
	3. Positions for Neon in Tungsten -----	24
	4. Positions for Argon in Tungsten-----	24
	5. Positions for Krypton in Tungsten-----	34
	6. Positions for Xenon in Tungsten -----	34
	7. Distance Ratios as a Function of Relative Masses -----	39
	B. DYNAMIC RUNS -----	39
	1. Survey of the Possible Directions of Escape For the Ar-W Simulated Split Interstitial in Site A-89 -----	39

2. Determination of Simulated Binding Energy

of Argon In Site A-89-----42

VI. CONCLUSIONS-----43

APPENDIX A: COMPUTER PROGRAM GLOSSARY-----45

COMPUTER PROGRAM-----52

BIBLIOGRAPHY-----65

INITIAL DISTRIBUTION LIST-----67

DD FORM 1473-----68

LIST OF TABLES

I.	Theoretical and Simulated Split Interstitial	
	Distance Ratios-----	40
II.	Detailed Impact Point Testing-----	42

LIST OF FIGURES

1.	Split Interstitial Sites for BCC Tungsten -----	19
2.	A,C Sites for Atoms 64, 114 - Helium-Tungsten-----	25
3.	A,C Sites for Atoms 89, 139 - Helium-Tungsten-----	26
4.	B Sites for Atoms 64, 89, 114, 139 - Helium-Tungsten---	27
5.	A,C Sites for Atoms 64, 114 - Neon-Tungsten-----	28
6.	A,C Sites for Atoms 89, 139 - Neon-Tungsten-----	29
7.	B Sites for Atoms 64, 89, 114, 139 - Neon-Tungsten----	30
8.	A,C Sites for Atoms 64, 114 - Argon-Tungsten-----	31
9.	A,C Sites for Atoms 89, 139 - Argon-Tungsten-----	32
10.	B Sites for Atoms 64, 89, 114, 139 - Argon-Tungsten----	33
11.	A,C Sites for Atoms 64, 114 - Krypton-Tungsten-----	35
12.	A,C Sites for Atoms 89, 139 - Krypton-Tungsten-----	36
13.	B Sites for Atoms 64, 89, 114, 139 - Krypton-Tungsten--	37
14.	C Site for Atom 89 - Xenon-Tungsten-----	38
15.	Impact Area - Dynamic Simulation of Escape Directions for Argon in Site A-89-----	41

ACKNOWLEDGEMENT

I wish to express my appreciation to Prof. Don E. Harrison, Jr., for his guidance and understanding during this project. I also wish to thank my wife, Margaret Ann, for her perserverence throughout the project and for her help in preparing the figures used in the text.

I. INTRODUCTION

The advent of modern, high speed digital computers has led to the application of computer simulation techniques to many different types of physical systems. One such application is the modeling of the situation that occurs when a foreign atom interacts with a metallic crystal lattice. In general, such modeling can be broken down into two basic areas, dynamic simulation and static simulation. As an example of the former, radiation damage has been studied by the simulated firing of an atom or ion onto a crystal face. Other examples are sputtering simulations [1,2,3] in which the incoming particle causes surface atoms to be ejected; and channeling simulations [4] in which the ranges of ions travelling in crystal lattices are calculated. Static simulations, on the other hand, have been concerned with the equilibrium positions in the lattice after point defects such as replacement atoms, interstitial atoms, and vacancies have been introduced. Examples of this type of simulation can be found in [5,6,7]. This present research utilized aspects of both static and dynamic simulation techniques. The goal of this research was to correlate the results of experimentally determined binding energies of point defects in a tungsten lattice [8,9] with the results obtained by computer simulation.

II. NATURE OF THE PROBLEM

A. HISTORICAL BACKGROUND

An investigation of radiation damage events by computer simulation techniques of crystalline behavior was published in 1960 by Gibson, Goland, Milgram, and Vineyard, hereafter referred to as (GGMV) [5]. This Brookhaven National Laboratory investigation set forth the criteria that must be satisfied before the simulation method could be applied to crystals. Such factors as potential energy functions, forces, crystallite sizes, computation methods, choice of time intervals, and computer limitations were discussed. The crystal lattice modeled in their research was metallic copper, a face-center cubic (fcc) structure. The potential functions used in the calculations was a Born-Mayer repulsive potential, with the necessary cohesive forces applied on the boundaries of the crystallite. In integrating the equations of motion, the Brookhaven group used the central difference procedure. The optimum choice for timestep duration, Δt , was shown to be of critical importance in the integration scheme. The energy of the strongest interaction governed their choice of the above parameter. The static results obtained by GGMV confirmed the existence of the $\langle 100 \rangle$ split interstitial in the fcc lattice. Their dynamic results described collision chains and focusing phenomena in crystallites struck with energetic knock-on atoms.

Additional crystal simulation studies were performed by R.A. Johnson [6,10,11]. In Ref. 6, he investigated point defects in a copper lattice using Born-Mayer repulsive potentials. The

$\langle 100 \rangle$ split interstitial was found to be the only stable interstitial position. He found it necessary to allow the interstitial to interact only with its six nearest neighbors. Atoms near the defect were treated as independent, while the remainder of the metal was treated as an elastic continuum with atoms imbedded in it.

Research on body-centered cubic (bcc) crystals was undertaken by Erginsoy, Vineyard, and Englert (EVE) [7]. They used a composite potential function for most of their detailed work. It consisted of an exponentially screened Coulomb potential at small separations, a Born-Mayer function in the region between small and intermediate separations, and a Morse potential at larger separation distances. A split interstitial was reported for simulated bcc crystals in the $\langle 110 \rangle$ direction. In their dynamic results they reported the existence of a threshold energy for displacement that was highly independent of the direction of knock-on. Also, collisional chains in the $\langle 111 \rangle$ and $\langle 100 \rangle$ directions were found to exist. R.A. Johnson also published results for bcc simulations involving α -iron and tungsten [11]. The existence of the split interstitial in the $\langle 110 \rangle$ direction was confirmed and crowdion migration data were discussed. The present investigation confirmed the $\langle 110 \rangle$ split interstitial positions for argon, neon, krypton, and xenon.

D.E. Harrison and associates have published several articles in which computer simulation of crystalline behavior has been investigated [1,2,12]. In a study of a fcc model of copper, collision events between a copper atom and a copper lattice were

simulated as a function of the potential function, the energy of the collision, and the location of the impact point. The integration scheme used was an average force procedure, instead of the central difference procedure used by GGMV. A complete discussion of the method can be found in Ref. 13. A continuation of copper simulations was published by Harrison, Leeds, and Gay in 1965 [12]. Another paper by Harrison and Greiling dealt with the ranges of heavy ions in tungsten crystals whose atoms had undergone thermal displacement [4]. It was found that room temperature thermal displacements had a negligible effect upon the collisions for ion energies greater than a few thousand electron volts. Finally, Harrison, Levy, Johnson, and Effron published results on computer simulation of sputtering [2].

Research undertaken by Vine [14] provided the foundation for this author's present investigation. Vine used the Gay-Harrison model for crystal simulation as modified by Levy [15], Johnson [16], Effron [17], and Moore [18]. His overall objective was to correlate experimental and simulated binding energies of neon and argon point defects. Repulsive potential functions for neon-tungsten (Ne-W) and argon-tungsten (Ar-W) interactions were used [19]. Morse functions were not used for those interactions because experimental data giving the Morse parameters was based on homogeneous media such as tungsten-tungsten (W-W) interactions [20]. Vine subsequently attempted to correlate results of equilibrium position studies for tungsten defects in a tungsten lattice using two different potential functions for the interstitial-lattice interactions. In one case, the tungsten interstitial was allowed

to interact using a Born-Mayer repulsive potential, and the other case, the tungsten defect was given a composite potential that was identical to that given to all the other lattice atoms. By so doing, he attempted to establish an empirical relationship between the two methods to apply to the results of neon interstitial studies which used only a repulsive potential.

The results of the tungsten-tungsten interactions failed to provide the information needed to formulate a correction factor to be used in the neon-tungsten studies. In addition, the concept of relating the potential energy at equilibrium to the experimentally observed binding energies of Kornelsen and Sinha [9] does not appear to be feasible.

B. CHOICE OF POTENTIAL FUNCTION

The studies that were reviewed in the previous section utilized many different approximations to the true potential function between atoms in a metal lattice. The problem of solving the many-body interaction of a real system is approximated in the computer by many two-body interactions. Thus, central pairwise potential functions are most often used in computer simulations. GGMV employed a repulsive potential of the Born-Mayer form:

$$V_{ij} = \exp(A + Br_{ij})$$

which described the repulsion of atoms at close approach. Three Born-Mayer potentials were investigated by GGMV to determine which would give the best results in their calculations. Their choice was one which has since been labeled the Gibson Number Two Potential. In Ref. 6, Johnson and Brown used a similar Born-Mayer potential

with slightly different parameters. As previously mentioned, another potential function that has been used in crystal modeling studies is the familiar Morse potential of the form:

$$\Phi_{ij} = D \left[\exp \left\{ -2\alpha (r_{ij} - r_0) \right\} - 2 \exp \left\{ -\alpha (r_{ij} - r_0) \right\} \right]$$

where r_0 is the equilibrium distance of approach of two atoms, and α and D are constants.

Girifalco and Weizer calculated Morse parameters that would be appropriate for several crystal lattices [20]. In calculating the parameters, they attempted to express the various crystal properties such as cohesive energy, lattice constant, compressibility and equation of state in terms of the Morse function. The Morse potential constants published by Girifalco and Weizer have been used extensively in simulating the potential functions and forces in lattices of homonuclear atom systems.

The Born-Mayer potential and the Morse potential are useful over specific internuclear separation distances. The Born-Mayer potential is useful at strongly repulsive separations, i.e. short ranges, while the Morse function is applicable at equilibrium and greater separations. In order to better approximate the true potential function, various investigators have combined different potential functions. As mentioned earlier, EVE [7] used a composite potential that consisted of an exponentially screened Coulomb potential at very close separations, a Born-Mayer potential at weakly repulsive distances, and a Morse potential over the remainder of the potential curve. In their studies, Harrison and associates combined a Born-Mayer potential and a Morse

potential. These two potentials were joined by a cubic equation in the region near their intersection [1,2,3,4].

C. EXPERIMENTAL RESULTS OF KORNELSEN AND SINHA

In 1968, Kornelsen and Sinha [7,8] published results concerning the binding energies of trapped particles such as neon, argon, krypton, and xenon ions in a tungsten surface. The particles were forced into the surface from a beam created by an ion gun which gave ion energies of 40 eV to 5 keV. The tungsten crystal was then heated and the rates of evolution of the trapped gas were measured.

The temperature at which desorption peaks occurred thus gave an indication of the binding energies of point defects in the tungsten crystal. Quantitatively similar results were obtained with argon, krypton, neon, and xenon ions. Four peaks were observed below 1650 °K and were labeled as α peaks. A single peak above 1700 °K was measured and was called the β -peak. It was concluded that the α -group of peaks were the results of single step desorptions from sites very close to the metal surface. They further concluded that the different α -peaks could correspond to different types of point defect binding energies in the tungsten crystal. Specifically mentioned were defects of three types; (a) interstitial and substitutional positions in the lattice, (b) different distances from the site to the surface, and (c) different locations of a nearby lattice defect, such as a vacancy, relative to the site and the surface.

III. THE SIMULATION MODEL

A. THE CRYSTAL

The model used in this research was essentially the same one used by Vine [14] as explained in Section II. In subsequent discussion, when it is necessary to specify certain of the computer program variable names, they will be placed in braces.

All of the simulations in this research were done with tungsten crystals of varying sizes. The objective was to use the smallest crystal dimensions that would give realistic results. The dimensions described below refer to the number of planes of atoms in each of the three rectangular coordinate directions. Simulations were performed with sizes $8 \times 6 \times 8$ of 96 atoms, $10 \times 6 \times 10$ of 150 atoms, $10 \times 8 \times 10$ of 200 atoms, and $10 \times 10 \times 10$ of 250 atoms. Of these, the latter two were judged to be of most use because of their greater depth in the y-direction. The y direction was always used as the direction of escape for the point defect atom.

Each atom in the simulated crystal was numbered, with the first position always assigned to the point defect atom. The remainder of the positions were assigned in sequence according to the coordinate locations. The numbering was started in the $y = 0$ plane and continued until all the atoms in that plane were specified. This procedure was repeated for the remainder of the y planes in the simulated crystal.

B. THE TIMESTEP INTERVAL

The numerical method of time integration used in the model was the average force method [13]. The value of Δt {DT} used in this procedure was of critical importance in determining whether or not the model would approximate reality. Also, the program running time was a function of the timestep duration.

In order to best approximate reality, the {DT} was kept smaller early in the program when most movement was expected, and was allowed to grow larger as equilibrium was approached. The parameter that controlled the timestep duration was {DTI}, the distance which the most energetic atom was allowed to move in a single timestep. In previous work, {DTI} was held constant throughout the duration of a program. If the motion was expected to be slow, {DTI} was given a larger value than in a situation where simulated motion was expected to be greater. For static equilibrium problems, at least 100 timesteps were needed to reach an approximately stable position. In addition, it became necessary to insert a maximum value for the timestep, {DT}, into the program to prevent unrealistic movement of the atoms and breakdown of the model.

In the current program, changes were made to allow {DTI} to decrease during the program. For example, in static runs on He-W, Ne-W, Ar-W, and Kr-W, {DTI} was initially given a value of 0.1 lattice unit {LU}. Tungsten forms a bcc crystal, with LU equal to $\frac{1}{2}LC$ or 1.58 \AA , where LC is the Lattice Constant or cube edge distance. {DTI} was allowed to change in decrements of 0.01 LU per timestep for the first 10 timesteps. Then the {DTI} value of 0.01 LU was allowed to change in decrements of .001 LU for

another 10 timesteps. Equilibrium was reached by 30 timesteps according to this procedure, resulting in a significant decrease of computer running time. Also, the equilibrium positions obtained in the simulation were closer to the expected $\langle 110 \rangle$ split interstitial positions than were obtained with a constant $\{DTI\}$ value.

IV. SIMULATION PROCEDURE

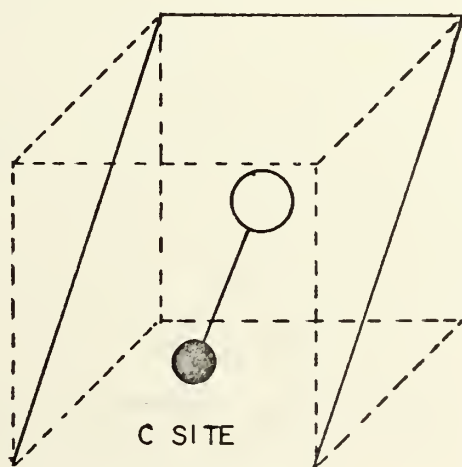
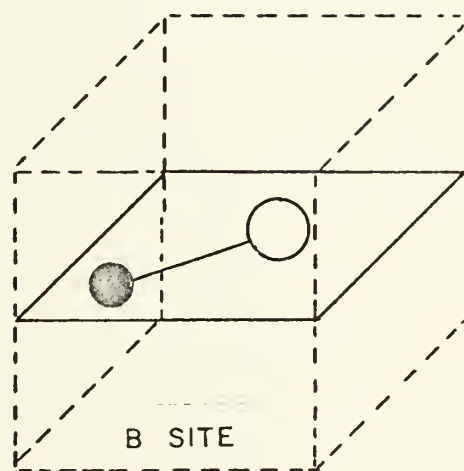
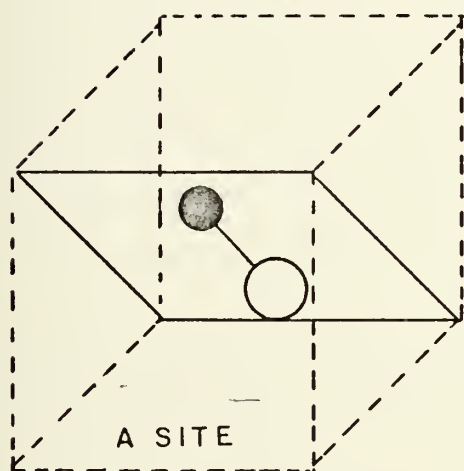
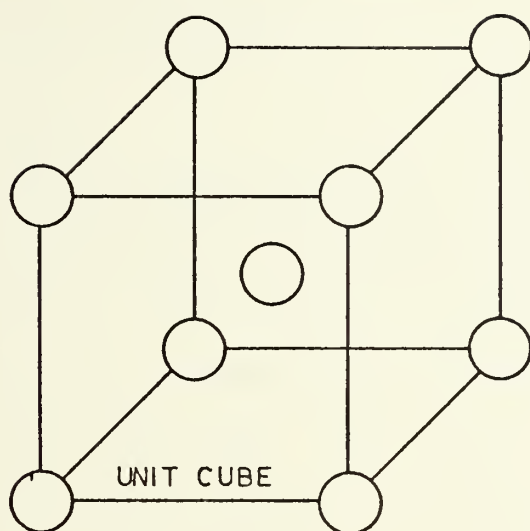
A. STATIC SIMULATIONS

The first stage of the simulation procedure was concerned with finding the equilibrium positions for the point defect of interest in the top several layers of a bcc tungsten crystal. Previous work done by Johnson [11], indicated that a bcc crystal had at least two different types of stable split interstitial orientations. The first of these was in a $\langle 100 \rangle$ direction along a (110) plane. The other stable orientation was in a $\langle 110 \rangle$ direction in a (100) plane. An analysis of the total of 12 stable split interstitial positions possible about a given atom in the two orientations listed above, revealed that there were only three independent types of sites. (See Figure 1.) The first of these is located on a (110) plane with {NVAC} and lies closer to the surface than {NVAC}. The second independent position lies in the same (100) plane as {NVAC} and is at the same depth in the crystal. A final position similar to the first, in that it is along a (110), is located at a depth below that of {NVAC}. The three different split interstitials were postulated to have different binding energies because of their varying depths in the crystal.

In order to reduce the running time in locating the final coordinate positions at each interstitial location, the static programs were started with the foreign atoms in the approximate area of the expected final positions as discussed above. For

Figure 1

SPLIT INTERSTITIAL SITES FOR BCC TUNGSTEN



example, when it was desired to locate position A, the foreign atom was initially placed along the correct (110) plane approximately one lattice unit from {NVAC}.

B. DYNAMIC SIMULATIONS

The dynamic simulation program used the final positions computed in the static programs as input initial crystal positions. The lattice generator subroutine {B100}, and the point defect locator {PLACE} were thus eliminated from the dynamic program.

Dynamic simulations were broken down into two main categories. The first category consisted of survey runs of the areas above the interstitials in the direction of escape from the y surface. An impact point generator package was inserted into the dynamic program, thus permitting the interstitial to be directed at a specific number of locations in a predefined area. The results of the survey run were analyzed to determine the optimum aiming point for the interstitial at a specific initial energy. It was observed during the impact testing procedure that the "best" aiming points were a function of the initial energy given to the interstitial. However, it was also found that the optimum aiming points at varying energies were in a generally localized area. Thus, once the optimum points were found at the starting energy, only a localized region around those points was tested at lower initial interstitial energies. The decrementing process of the initial interstitial energy constituted the second main phase of the dynamic simulations. The procedure in this phase was to decrease the interstitial energy until it could no longer escape

from the crystal. The minimum escape energy was said to be the simulated binding energy of the interstitial at the particular location tested.

V. PRESENTATION OF DATA

A. STATIC RUNS

1. Preliminary Testing of Static Program

One hundred twelve computer runs were made in the initial testing phase of the static program. The bulk of the testing was done in four general areas: 1) Program shutdown procedures at equilibrium; 2) Optimum crystal size determination; 3) Equilibrium position as a function of the initial interstitial position; and 4) Realistic timestep determination procedure.

The best method of stopping the program at equilibrium has been a matter of concern for many years with the static simulation program. In the present investigation, the first method tested was a shutdown procedure initiated whenever a sharp {DT} decrease was encountered in the program. This test proved to be of limited success, and was later abandoned. Another method that was attempted was a test of {EMAX} against a value such as .04, to determine if equilibrium had been reached. This method also proved only partially successful. Finally, a test was made of the average kinetic energy of an atom in the simulated crystal. The average energy was taken to be the total kinetic energy {TPKE} divided by the number of atoms {LL}, or equivalently, {TPKE} multiplied by the reciprocal of the number of atoms {RLL}. The crystal was assumed to be at equilibrium if the average kinetic energy of an atom was less than or equal to the value 0.025 eV, a value for the average thermal energy of an atom. Satisfactory results were

sometimes obtained by this method but the test had to be removed in many cases to allow the simulated crystal to run a greater number of timesteps and reach equilibrium.

As previously mentioned, different sizes of crystals were simulated to determine the optimum dimensions for the crystallite. Many tests were made on crystal sizes smaller than the $10 \times 10 \times 10$ used by Vine [14]. Although smaller sizes such as $10 \times 6 \times 10$ often gave reliable results, it was finally decided to use the $10 \times 10 \times 10$ size for the reported split interstitial positions in order to have a standard size applicable over all crystal positions of interest.

In his work, Vine placed his interstitials in the middle of the open channels in the simulated crystal. Numerous runs in the present research have indicated that equilibrium is reached more quickly when the initial starting positions are not in channel centers, but along the directions of the expected splits in the general area of the final positions.

All of the initial work was done with a fixed $\{DTI\}$ value in the program. The $\{DTI\}$ value normally used was .05 LU. The timestep interval was later modified as explained in The Simulation Model and the computer running time was cut by approximately two-thirds due to this procedure.

2. Positions for Helium in Tungsten

Helium was the lightest point defect used in the static simulation model. It was thought that the small, light atom would essentially do all the movement and come to rest in a channel center $\sqrt{2}$ LU away from $\{NVAC\}$ along the $\langle 110 \rangle$ direction. The results of the runs show that the movement was almost as expected.

Also, a comparison of the C site for atom 64 and the A site for atom 114 indicates that there is a strong possibility that these two sites are degenerate. This is based on the fact that the potential energies of both sites are close, and also that the {NVAC} for each site is displaced only a negligible distance. The same probability of degeneracy is also seen to exist for C-89 and A-139. The determination of degeneracy of sites is seen to be a complex evaluation of potential energy differences, movements of {NVAC}, and the potential gradient between the two sites. The final positions for the A, B, and C split interstitial positions in the third, fourth, fifth, and sixth layers where {NVAC} was 64, 89, 114, and 139 respectively are shown in Figures 2, 3 and 4. The results obtained with helium were thought to be somewhat in error, since the heavier atom, neon, moved further in its simulations than helium. Further work is needed to confirm the equilibrium positions for helium.

3. Positions for Neon in Tungsten

The neon split interstitial locations were simulated for the same positions as helium. (See Figures 5, 6 and 7.) Essentially, the {NVAC} atom remained in its lattice site and the neon moved along a $\langle 110 \rangle$ direction to a distance $\sqrt{2}$ LU away from {NVAC}.

4. Positions for Argon in Tungsten

The bulk of the testing of this research was done with argon as the simulated point defect. The results of the runs for the 10 x 10 x 10 crystal size are shown in Figures 8, 9 and 10.

Figure 2

A & C SITES FOR ATOMS 64, 114

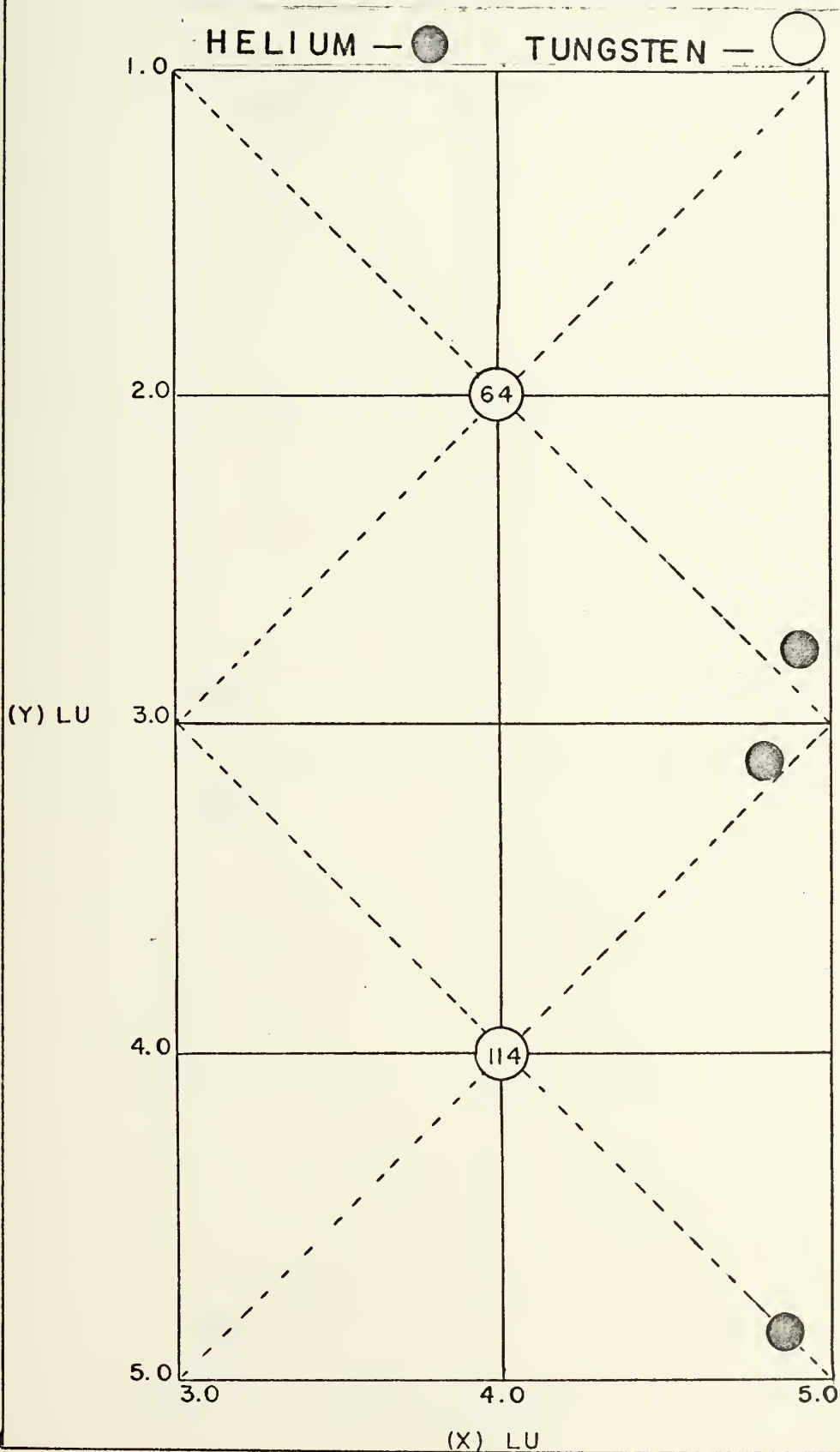


Figure 3

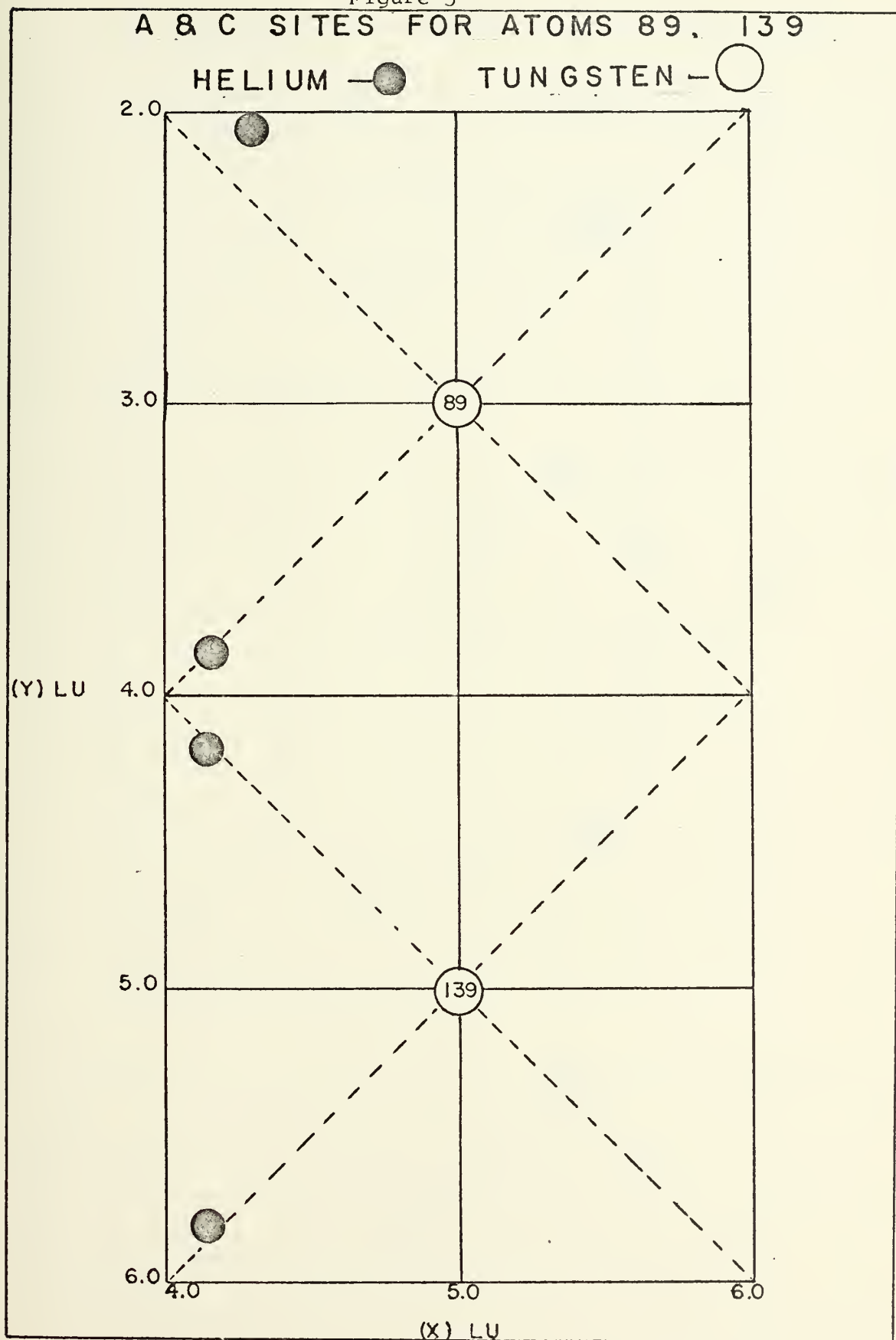


Figure 4

B SITES FOR ATOMS 64, 89, 114, 139

HELIUM — ●

TUNGSTEN — ○

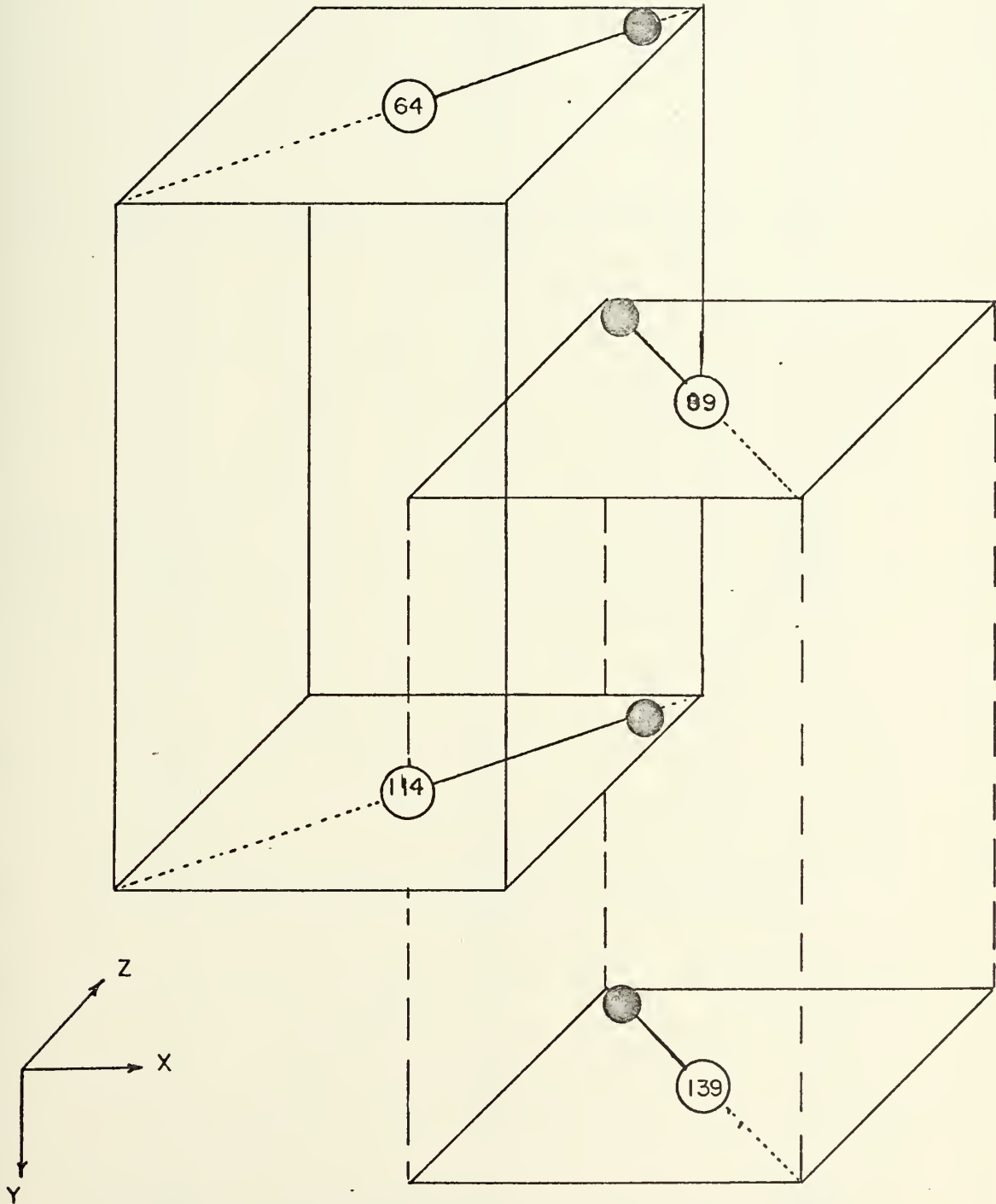


Figure 5

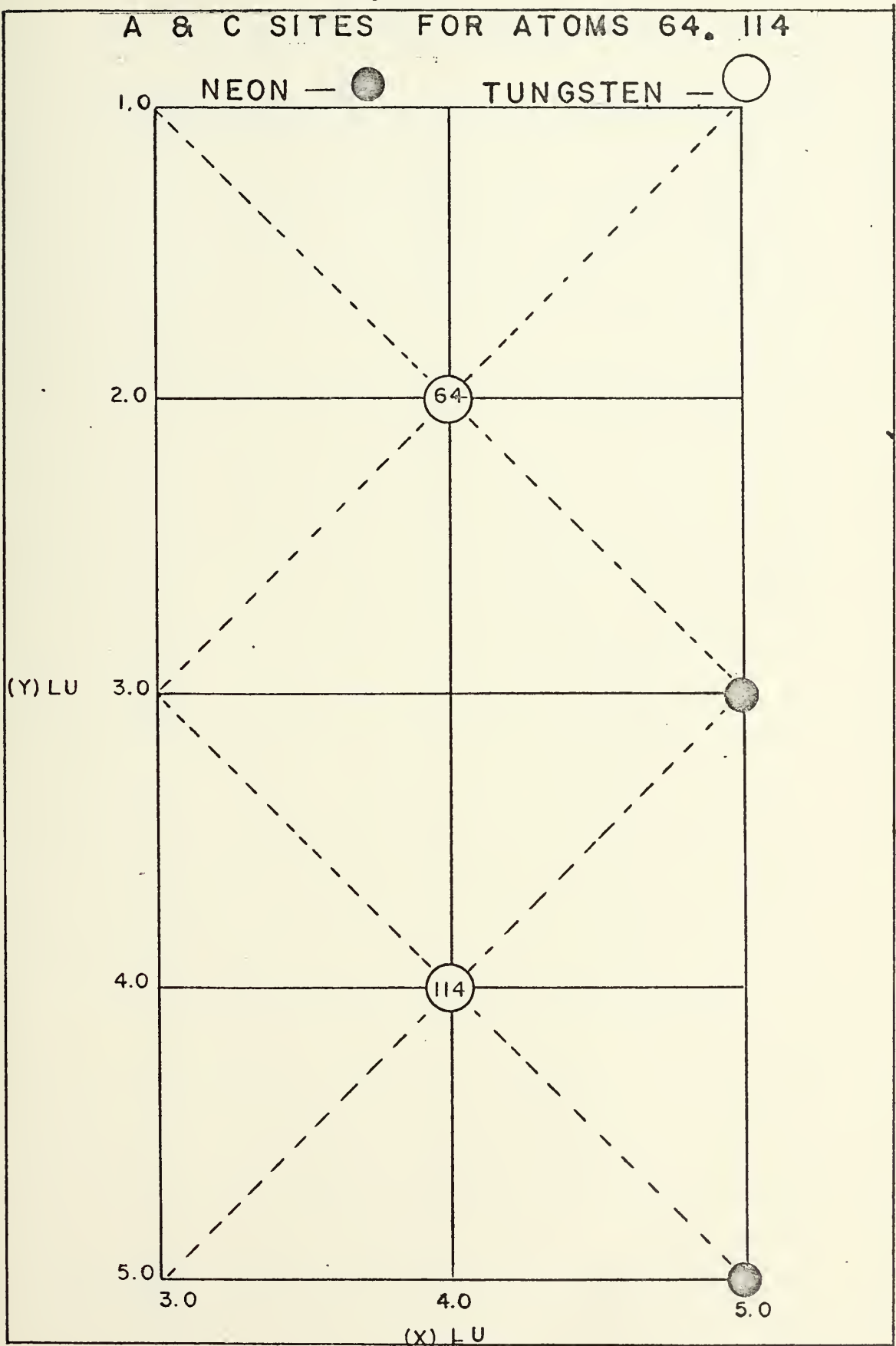


Figure 6

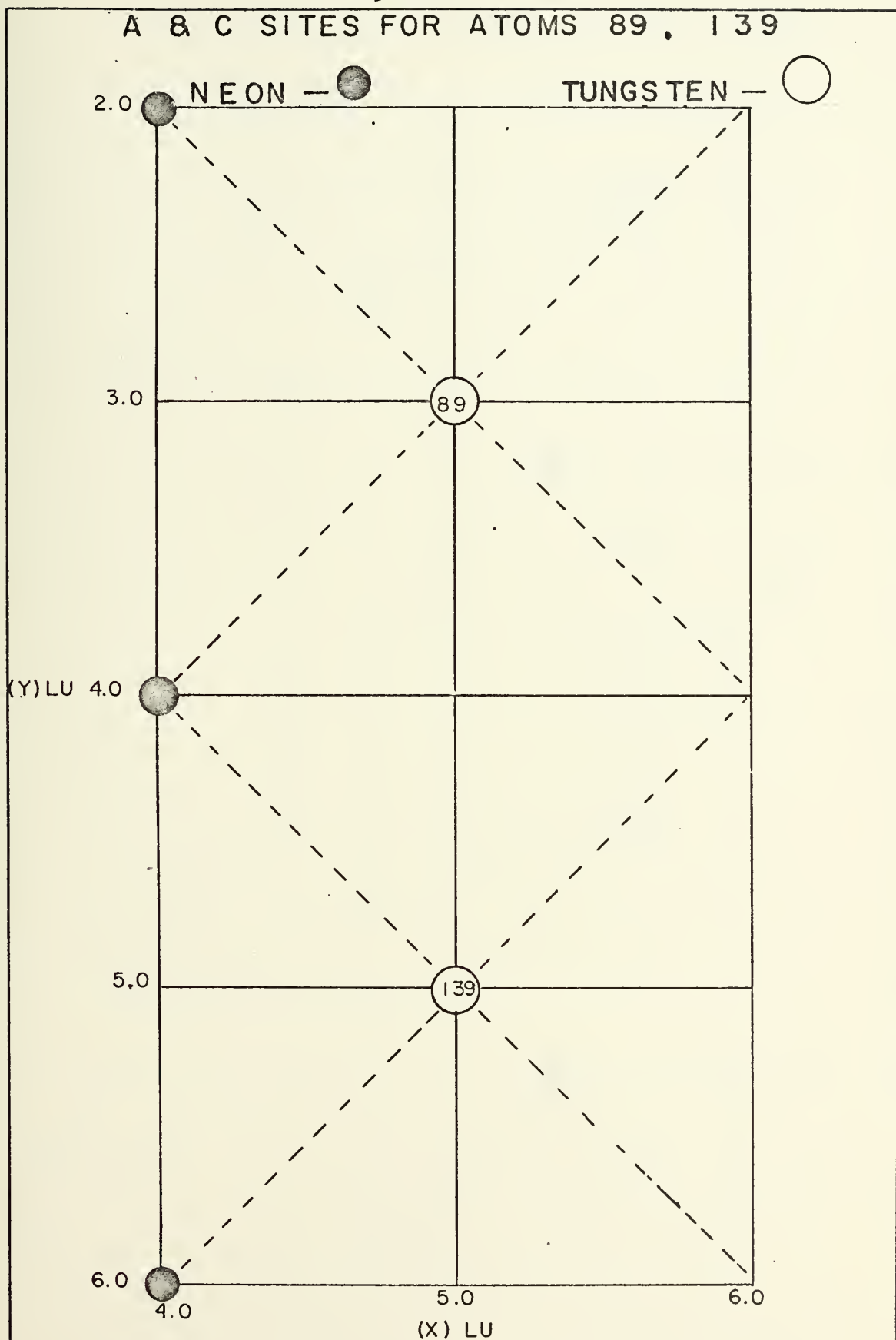


Figure 7

B SITES FOR ATOMS 64, 89, 114, 139

NEON —●

TUNGSTEN —○

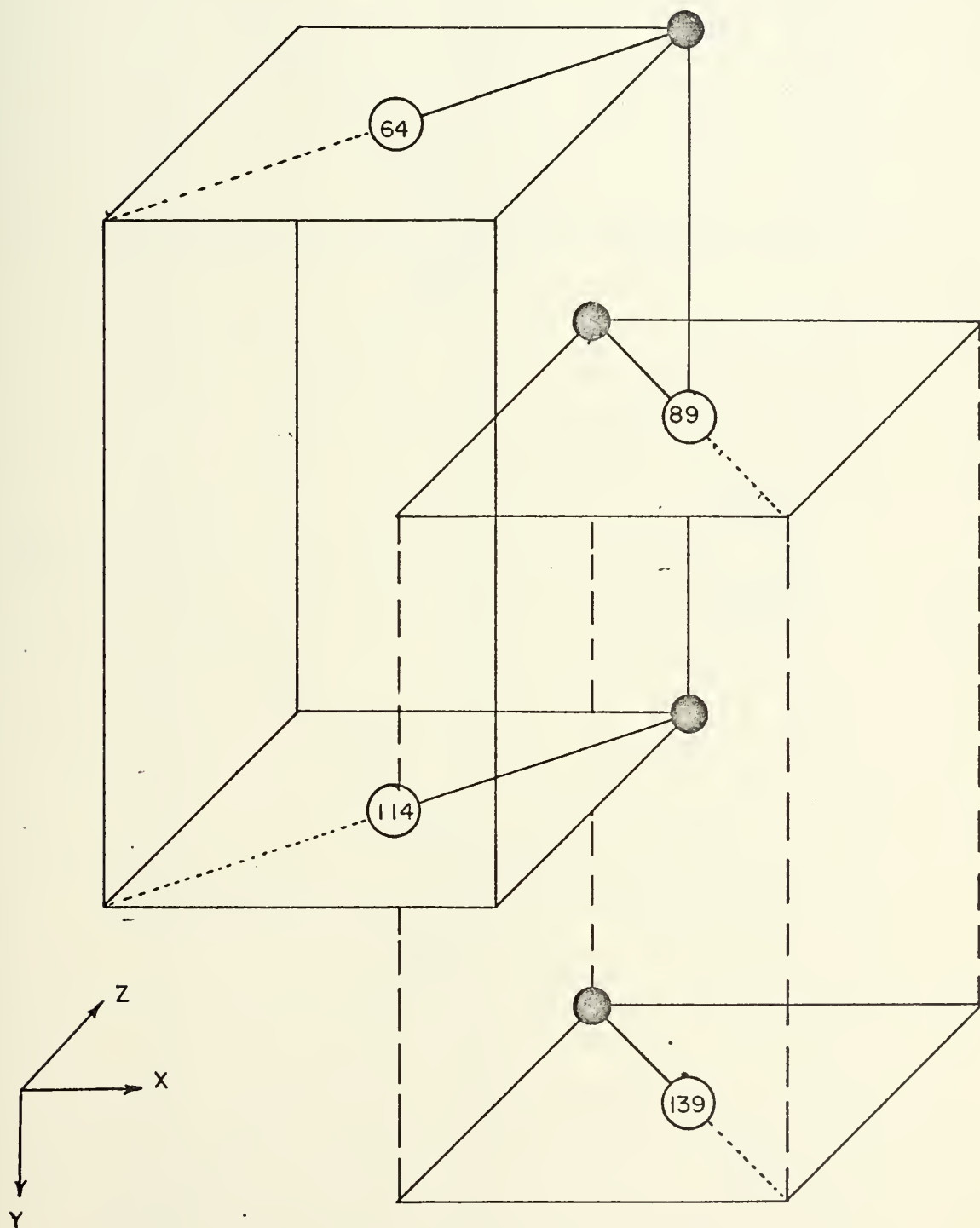


Figure 8

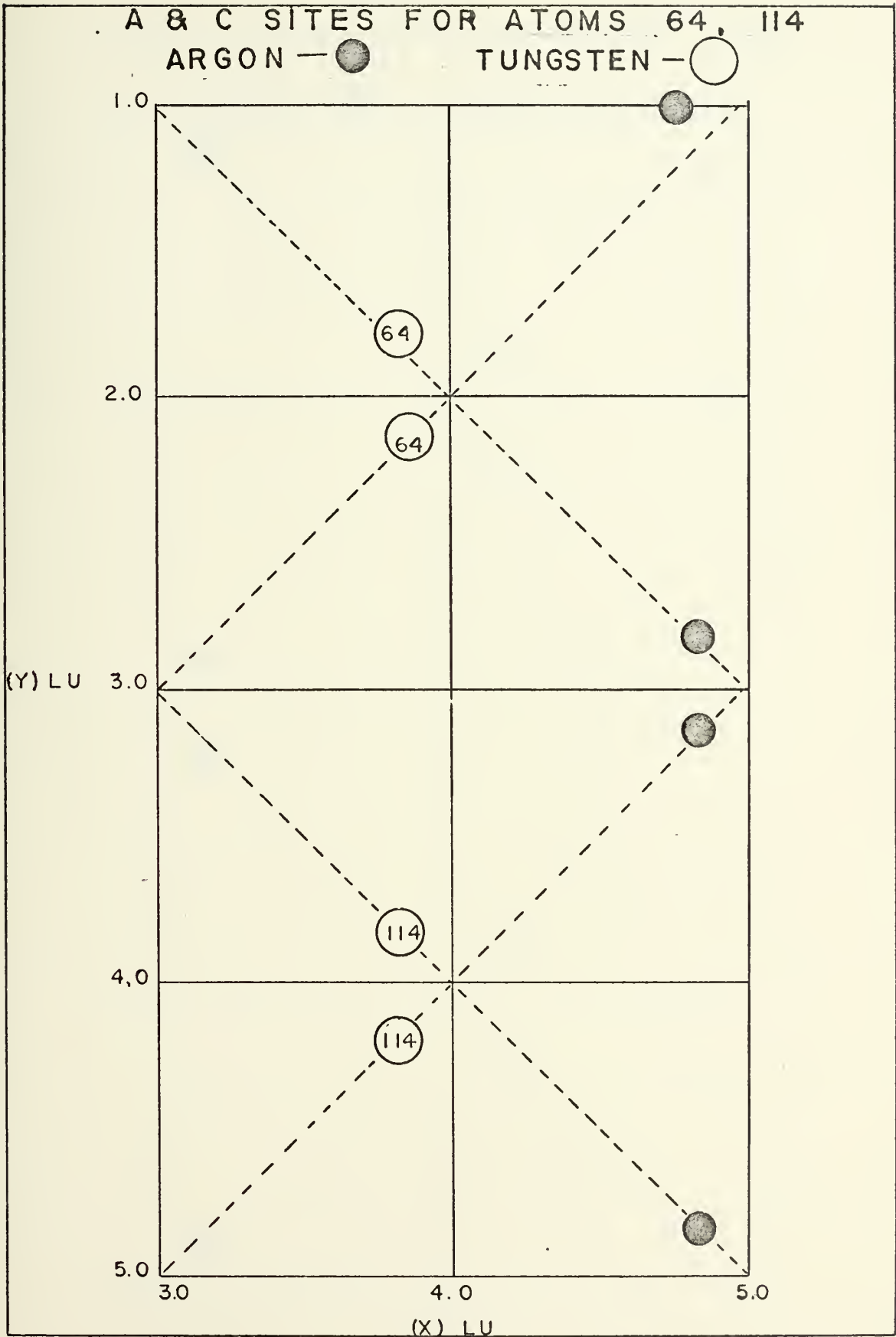


Figure 9

A & C SITES FOR ATOMS 89, 139

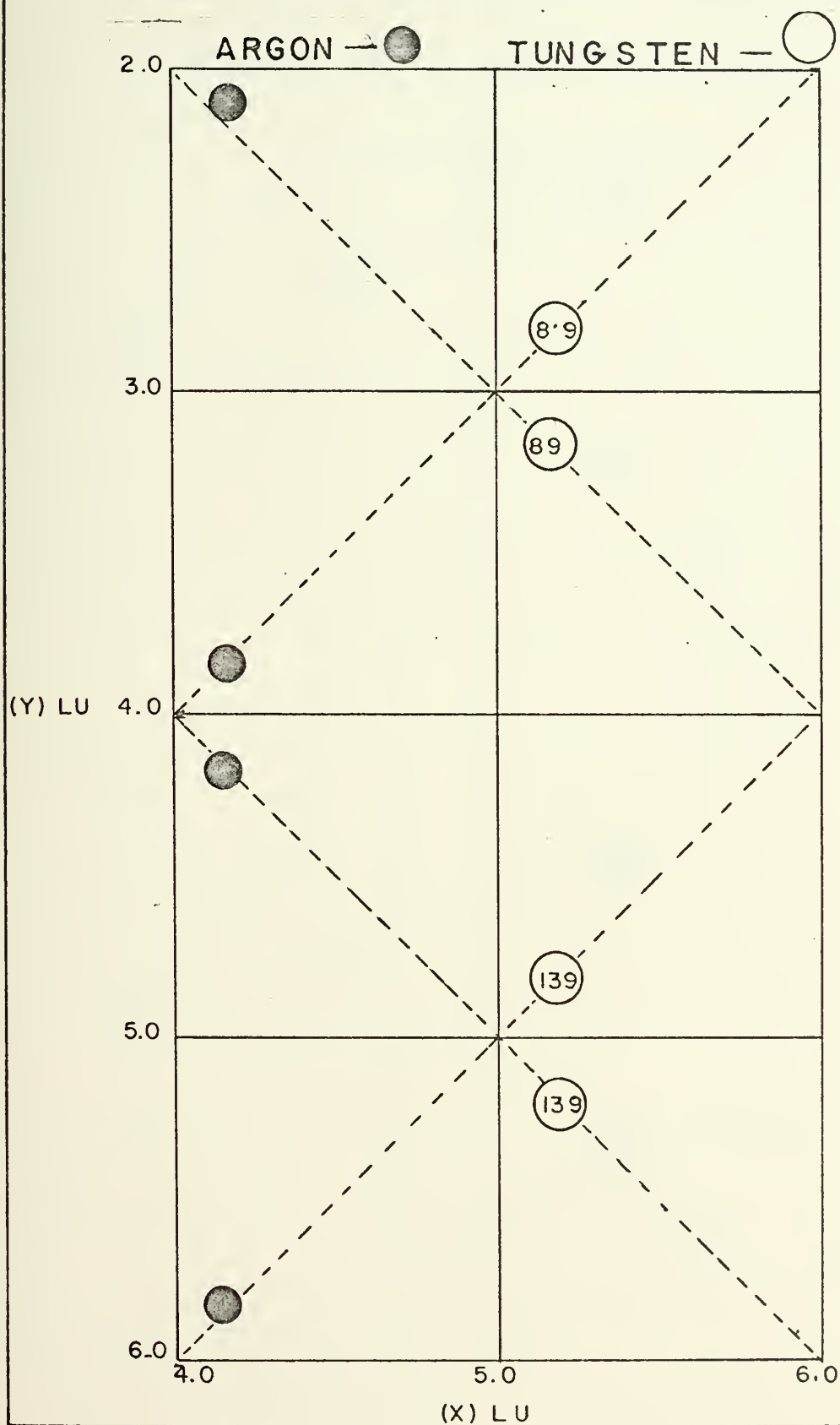
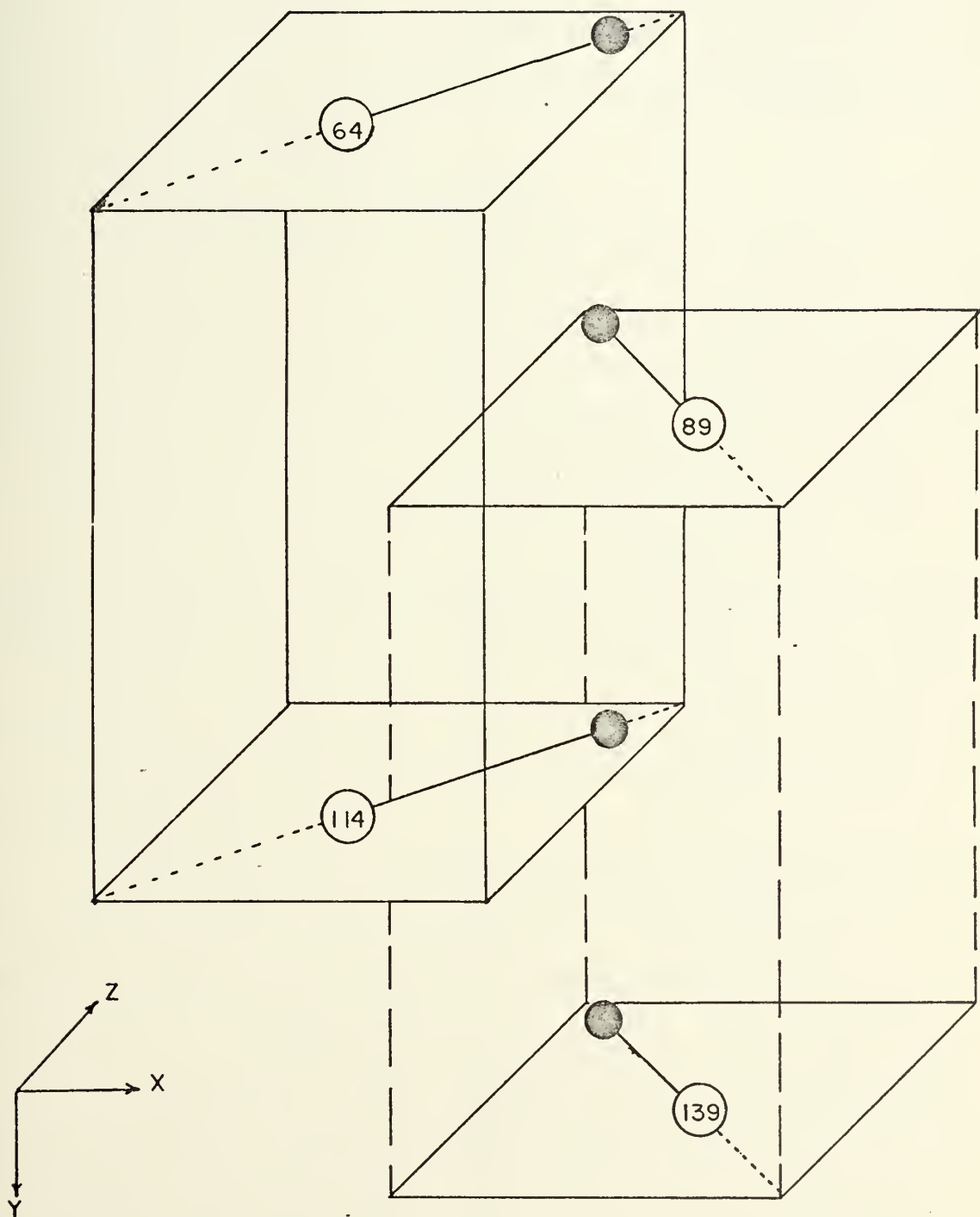


Figure 10

B SITES FOR ATOMS 64, 89, 114, 139

ARGON — ●

TUNGSTEN — ○



The expected $\langle 110 \rangle$ splits were observed with {NVAC} moving away from its site in relation to the final position of the argon defect.

5. Positions for Krypton in Tungsten

The split interstitial positions for krypton in a simulated tungsten crystal were also plotted. (See Figures 11, 12 and 13.) Once again, satisfactory results were obtained and the $\langle 110 \rangle$ splitting was observed.

6. Positions for Xenon in Tungsten

For the Xenon Runs, the tungsten repulsive potential function was used for the xenon potential. The initial runs, using the {DTI} employed for the other defects, failed to give the postulated split interstitial positions. At least two factors were seen to complicate the Xenon-Tungsten runs. Firstly, the mass of Xenon was approximately $6/7$ that of tungsten, so the lattice site would be shared almost evenly. This would mean that tungsten would have to move a significant distance from its lattice position. Secondly, the relatively large size of the xenon defect would require more movement of the surrounding atoms to accommodate the extra atom.

The {DTI} scheme was changed to allow for more movement of the atoms by allowing {DTI} to change in smaller decrements. Another method that was used was an initial displacement of both the xenon and the tungsten away from the lattice site. When both atoms were displaced, it became necessary to use an initial {DTI} of .05 LU or less. An average value of the C site for atom 89 was computed. (See Figure 14.) More work is needed to simulate all of the interstitial positions.

Figure 11

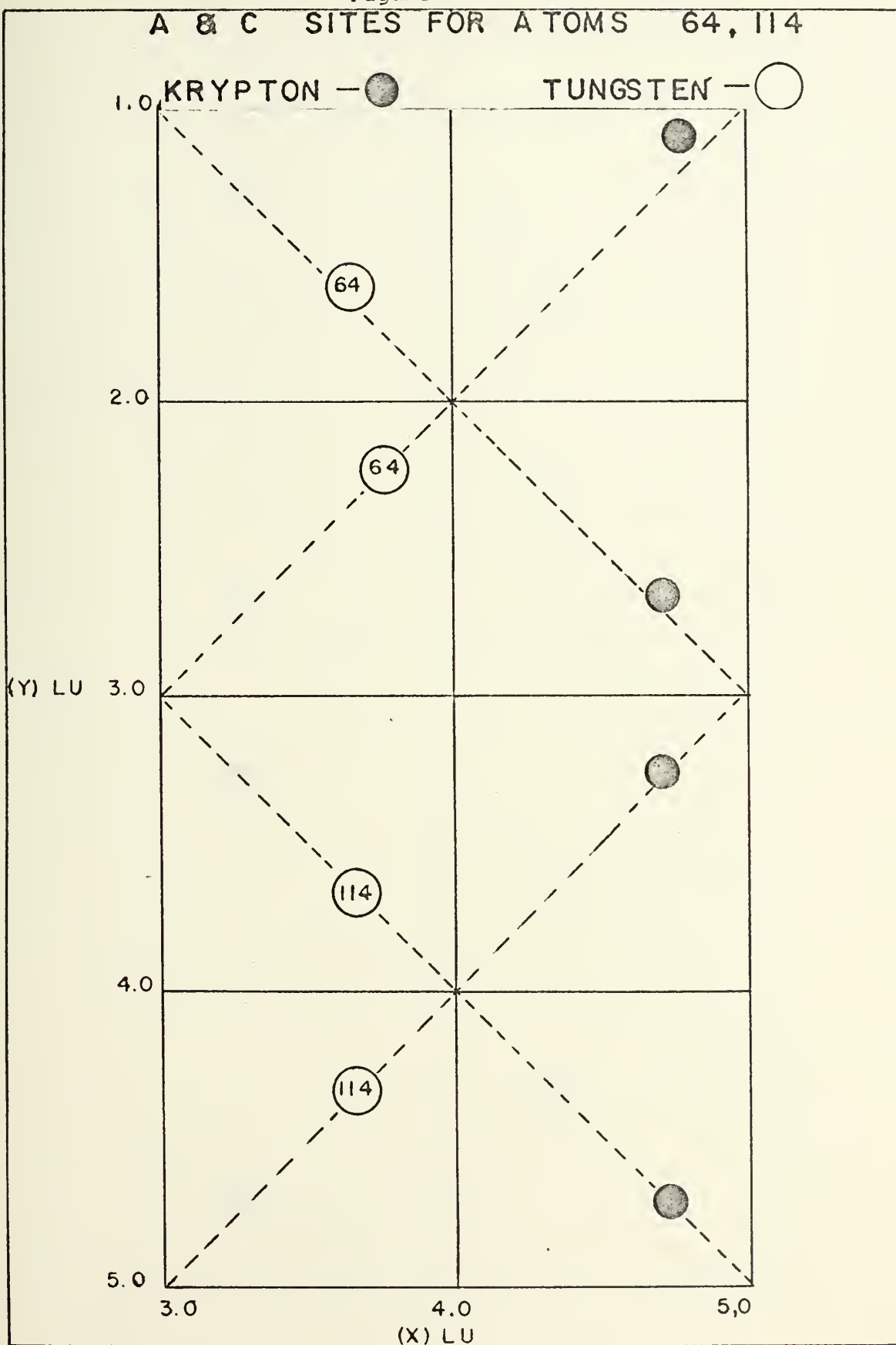


Figure 12

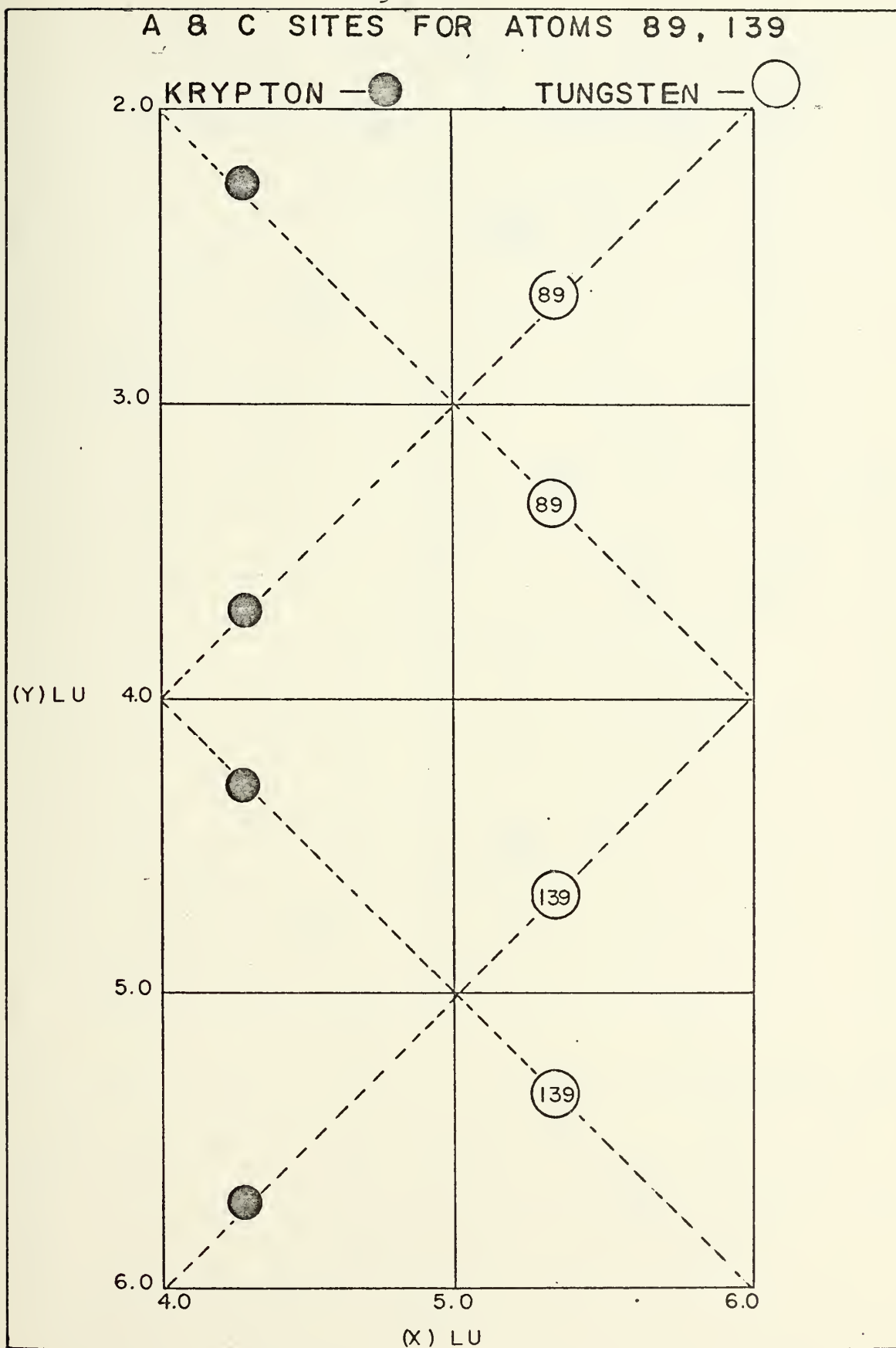


Figure 13

B SITES FOR ATOMS 64, 89, 114, 139

KRYPTON — ● TUNGSTEN — ○

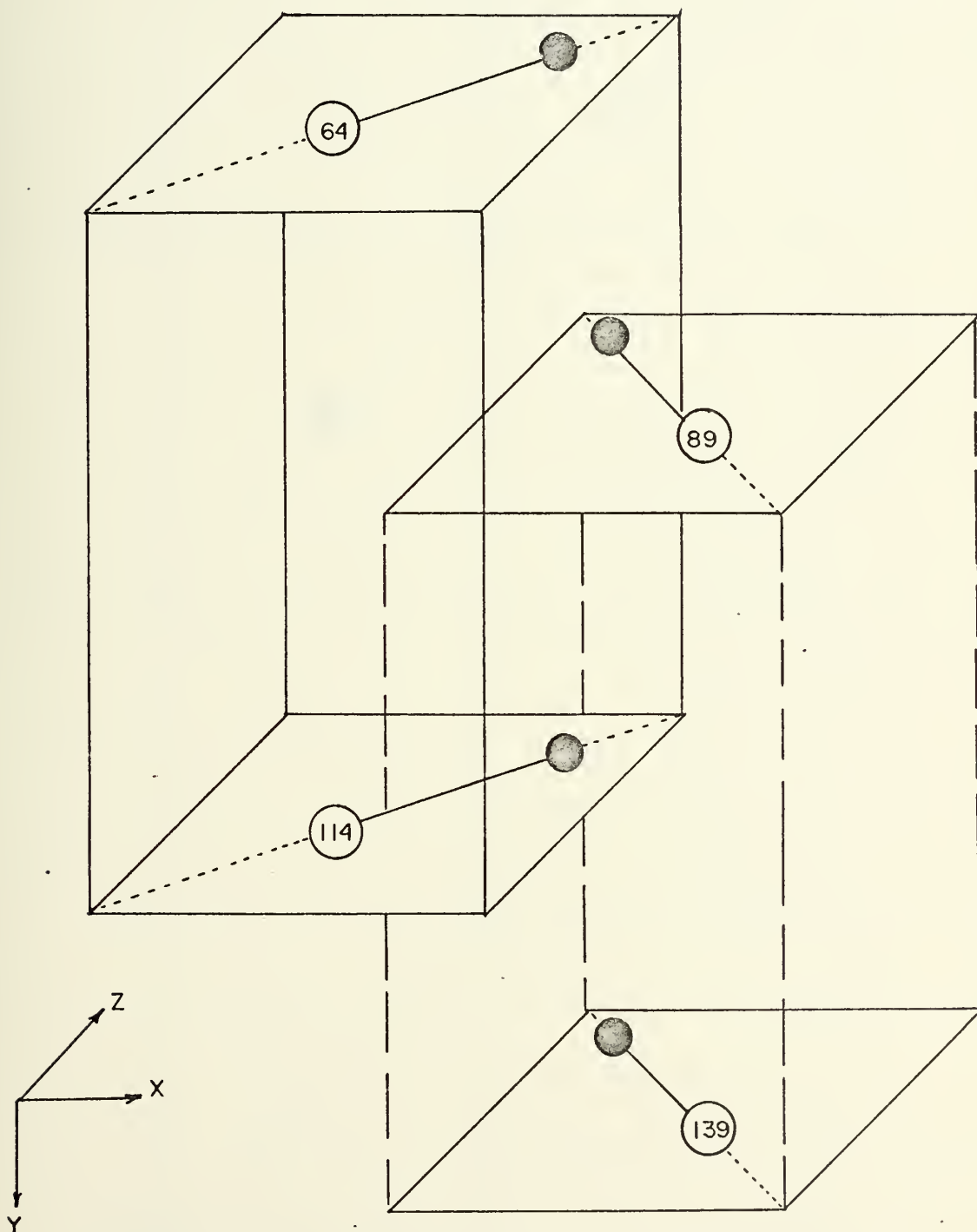
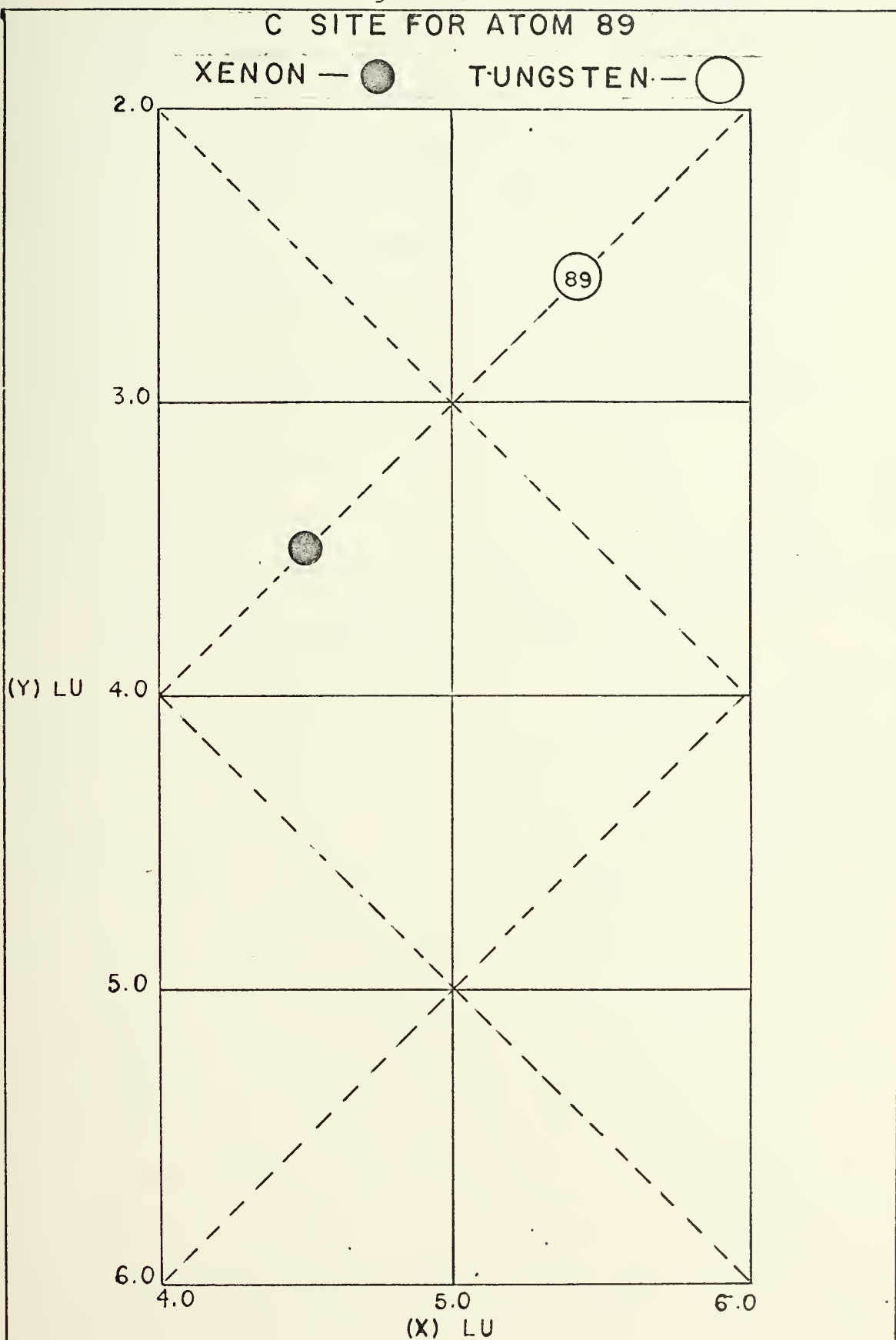


Figure 14



7. Split Interstitial Distance Ratios as a Function of Relative Masses

During the static testing phase, the ratios of the split interstitial distances from the initial {NVAC} were measured. An attempt was made to correlate these ratios to the inverse ratios of the atomic masses of the atoms involved. (See Table I.) The point defect results of helium and neon did not give any significant correlation, but the Argon and krypton atoms gave ratios of splits in good agreement with the expected values from mass ratio calculations.

B. DYNAMIC RUNS

1. Survey of the Possible Directions of Escape for the Ar-W Simulated Split Interstitial in Site A-89

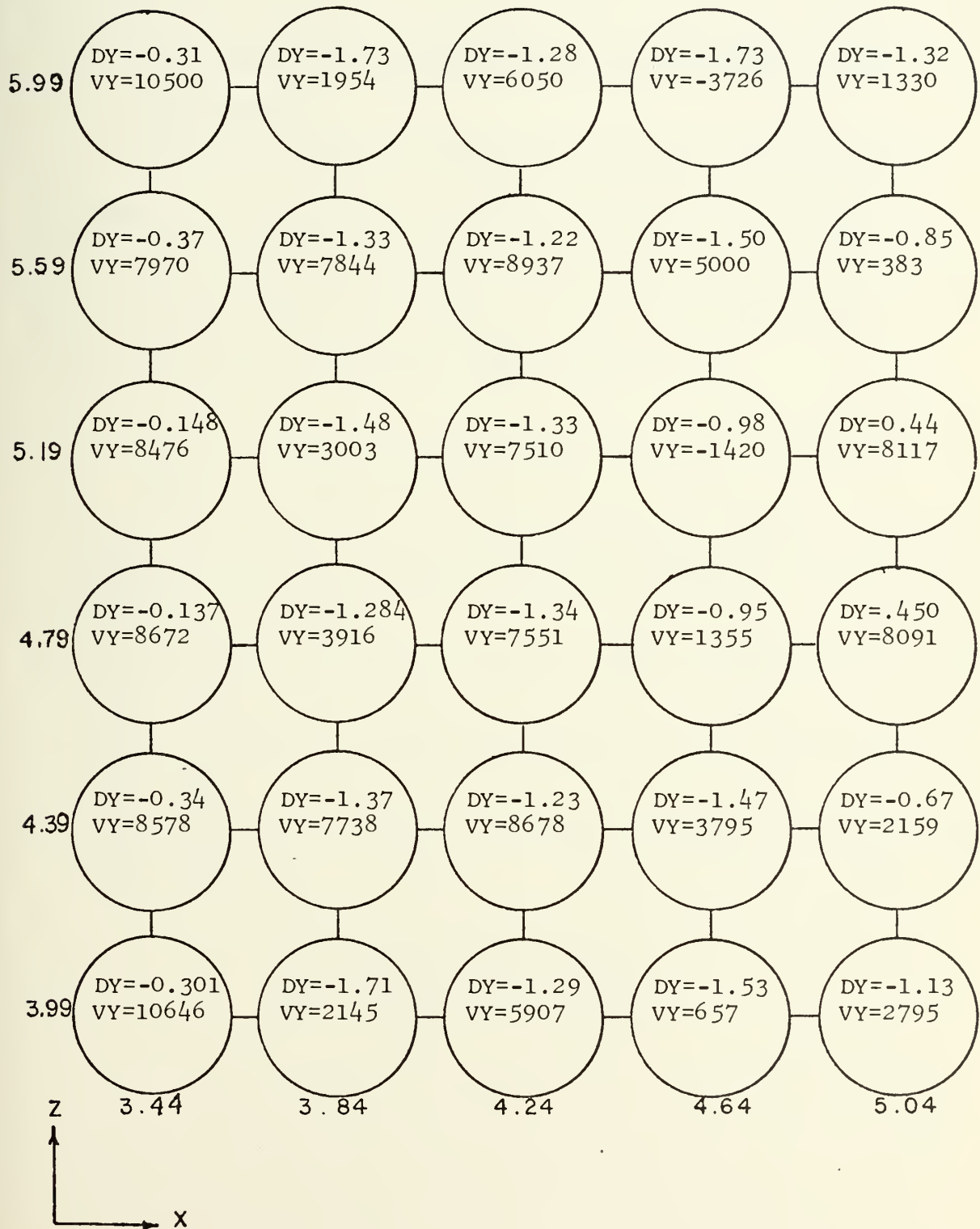
As was mentioned in the Section IV, survey runs were made of the possible escape directions in the plane one LU. above the defect. The results for the survey for the Ar-W split interstitial in site A-89 were plotted. (See Figure 15.) {DY}, the distance in lattice units that the argon moved in 25 timesteps, and {VY}, the velocity that the argon had after 25 timesteps are shown for each impact point. Due to the multiple scattering of the defect as it moved toward the surface, 25 timesteps were not sufficient to provide conclusive evidence at any one impact point. The survey was limited to 25 timesteps per impact point, however, due to computer time considerations. The main benefit gained from the survey run was the elimination of certain areas from further testing, such as those on the outer perimeter of the survey area. Also, much information was gained on the most likely area of escape for the

TABLE I

	Theoretical Splits From Lattice Site $\left(\frac{\text{Tungsten Mass}}{\text{Impurity Mass}} \right)$	Simulated Splits From Lattice Site $\left(\frac{\text{Impurity Distance}}{\text{Tungsten Distance}} \right)$
He-W	45.96	-----
Ne-W	9.11	-----
Ar-W	4.60	4.36
Kr-W	2.19	2.18
Xe-W	1.40	-----

Figure 15

IMPACT AREA : DYNAMIC SIMULATION OF ESCAPE DIRECTIONS FOR ARGON IN SITE A- 89



defect. From the results of the survey run, and from symmetry considerations of the open channel, it was decided to concentrate further testing on several points with the same Z coordinate as the interstitial atom.

2. Determination of the Simulated Binding Energy of Argon in Site A-89

Detailed testing of several impact points with the same Z coordinate as the argon was carried out for 100 timesteps per impact point. This was generally enough time for the simulated interstitial to escape the crystal if its initial energy was great enough. The results are summarized below.

TABLE II Detailed Impact Point Testing

Impact Points in Plane 1.0 LU in -y direction from Argon	Initial Energy				
	20 eV	10 eV	8 eV	6 eV	4 eV
CX = 3.84 LU CZ = 4.99	Yes	Yes	No	No	No
CX = 4.24 CZ = 4.99	Yes	Yes	Yes	Yes	No
CX = 4.44 CZ = 4.99	Yes	Yes	Yes	Yes	No

Yes - Atom Escapes Crystal

No - Atom Does Not Escape

VI. CONCLUSIONS

The method used to decrease $\{DTI\}$ on every timestep appears to be a significant improvement over the old method of keeping $\{DTI\}$ fixed. In effect, the new method forces the simulated crystallite to come to equilibrium in a predefined number of timesteps. In addition to a saving of computer time, this method also eliminates the need for a equilibrium shut down procedure in the program. The same $\{DTI\}$ decrement scheme could not be used for all the point defects tested in this research. For example, Argon and Krypton were able to come to their expected equilibrium positions using the scheme described in Section III, but Xenon and Helium were not. Thus it appears that defect size, as well as the expected degree of movement may dictate the $\{DTI\}$ decrement scheme.

The expected $\langle 110 \rangle$ split interstitials were confirmed for the helium, neon, argon, krypton, and xenon foreign defects. The relative degree of splitting does appear to be related to the masses of the interacting atoms, but conclusive evidence of this was only obtained for the Argon-Tungsten, and Krypton-Tungsten runs.

The dynamic runs have shown the direction of escape from the crystal to be a multi-collisional process, with the defect undergoing many intermediate direction changes at the low kinetic energies tested. The most likely escape direction was also seen to vary somewhat with the initial kinetic energy given to the defect.

The simulated value of approximately 4 eV for the binding energy of Argon in site A-89 appears to be a reasonable value. Kornelsen's data showed an energy level at this value and his levels were postulated to arise from defects in the first several layers of the tungsten crystal.

Further work is needed to confirm the remainder of the energy levels found by Kornelsen, by testing other point defect sites in the top layers of the simulated crystal.

APPENDIX A: COMPUTER PROGRAM GLOSSARY

NOTE: In this glossary, the terms "point defect atom", "bullet", and "primary" are synonymous; and the terms "latttice atom" and "target" are synonymous.

AC: Distance measurement used in impact point generator

ALPHA: Input Morse potential parameter

BSAVE: Target mass/(target mass + bullet mass); distributed potential energy between target and bullet

BIND: Negative of the total potential energy (TPOT) at time zero

EMAS: Mass of bullet in amu

BULLET: Alpha-numeric array for point defect material

CFO, CF1, CF2: Force parameters of cubic fit between Morse and Born-Mayer functions

CGB1, CGB2: Morse potential parameters

CGD1, CGD2: Morse potential parameters

CGF1, CGF2: Morse force parameters

COX, COY, COZ: Cosines of angles to x,y, and z axes respectively

CPO, CP1, CP2, CP3: Potential parameters of cubic fit between Morse and Born-Mayer functions

CVD: $\text{CVR} \times 10^{-10}$, converts lattice units to meters

CVE: 1.6×10^{-19} , converts electron volts to joules

CVED: CVE/CVD , a ratio used to avoid repeated division

CVM: 1.672×10^{-27} , converts atomic mass units to kilograms

CVR: LU in angstroms; converts lattice units to angstrom units

CX, CY, CZ: Coordinates of impact point

D1X, D1Y, D1Z: Displacement coordinates for location of interstitial from reference atom, NVAC

DCON: Input Morse potential parameter

DDTI: Time increment that is subtracted from DTI after each timestep

DDF: ROE-DIST, the distance closer than ROE that an atom is to the primary

DIST: Distance between any two atoms

DLPE: TLPE-TLPE \emptyset , the change in total local potential energy since time zero

DRX, DRY, DRZ: x,y,z components of DIST

DT: Length of a timestep in seconds

DTI: Number of lattice units most energetic atom may move in one timestep

DTIS: Starting value of DTI.

DTOD: DT/CVD--a ratio used to avoid repeated division

DTOM: DT/PTMAS--a ratio used to avoid repeated division

DTOMB: DT/PEMAS--a ratio used to avoid repeated division

DX(I), DY(I), DZ(I): Change in position of ith atom from initial position at time zero

EMAX: The maximum energy encountered in any cycle

ERAT: Measure of the average kinetic energy of an atom

EV: Primary energy in electron volts

EVR: Primary energy in kilo-electron volts

EXA, EXB: Input Born-Mayer potential function parameters for the target

F2: Square of the force on a specific atom
 FA: The component force increment on an atom
 FDTI: DTI X CVD, a parameter used to determine DT by maximum
 energy method
 FM: A small number used in checking potential energy zero
 point
 FM2: FM squared
 FMAX: Maximum total force on the most stressed atom in the
 crystal
 FMAX1: Maximum total force on Atom 1
 FOD: FORCE/DIST--a ratio used to avoid repeated division
 FORCE: Numerical value of the force function with a variable
 parameter
 FX(I), FY(I), FZ(I): x,y,z components of total force on an atom
 FXA: Born-Mayer force function parameter
 HBMA: $\frac{1}{2}$ BMAS-- a ratio used to avoid repeated division
 HDTOD: $\frac{1}{2}$ DTOD-- a ratio used to avoid repeated division
 HDTOM: $\frac{1}{2}$ DTOM-- a ratio used to avoid repeated division
 HDTOMB: $\frac{1}{2}$ DTOMB-- a ratio used to avoid repeated division
 HTMA: $\frac{1}{2}$ TMA-- a ratio used to avoid repeated division
 I1: Variable in cubic fit subroutine
 I3: Variable in cubic fit subroutine
 IDEEP: Number of mobile layers
 IH1: Alpha numeric array for program title
 IH2: Alpha numeric array for Morse function parameters
 IHB: Alpha numeric array for bullet element
 IHS: Alpha numeric array for type and orientation of crystal

IHT: Alpha numeric array for target element

ILAY: Same as IDEEP

IN: Odd-even integer used to determine atom site establishment

IP: Subscript value of atom. Used in subroutine STEP and ENERGY

IQ: Parameter that determines whether or not a self defect is to be given a repulsive potential or a composite attractive-repulsive potential

ISHUT: A parameter used to shut down the program

IT: Unscaled fixed point x coordinate used in lattice generation

ITT: Odd-even integer used to determine atom site establishment

ITYPE: Parameter used to determine the type of point defect: vacancy, self-interstitial, replacement, foreign interstitial

IVACX, IVACY, IVACZ: Input plane numbers to specify NVAC

IX, IY, IZ: Number of x,y,z planes of crystal

J2: Variable in the cubic fit subroutine

JT: Unscaled y coordinate used in crystal generation

JTS: Variable used to establish atom sites

JTT: Variable used to establish atom sites

KF: Final K in LOCAT (K) assigned to an atom

KT: Unscaled z coordinate used to establish atom site

LCUT(I): Used to identify an ith atom which is not included in calculations

LD: The highest numbered atom in the mobile layers

LL: The highest numbered atom in the entire crystal

LOCAT(K): Dimensioned variable that remembers the numbers of the atoms within a radius ROEL of the primary at time zero

LS: Variable associated with each of the nine lattice generator subroutines

MCRO: One number higher than the order of the fit between the Born-Mayer and Morse potentials, always 4 in this simulation

ND: Data output increment, in numbers of timesteps

NDEC: Counting index for DTI variation

NEW: Parameter used to determine whether or not atom numbers have been stored in LOCAT(K)

NPAGE: Page numbering variable

NRUN: Parameter used to determine whether or not to read additional data cards

NS: Initial print statement timestep number

NT: Timestep number

NTT: Timestep number limit before shutdown

NVAC: An atom number used to establish point defects or used as a reference point for interstitial placement

PAC: Parameter for bullet force function correction

PEMAS: Primary mass in kilograms

PEXA, PEXB: Input Born-Mayer potential function parameters for the bullet-target interaction

PFPTC: Primary force function evaluated at ROE

PFXA: Primary force function parameter

PKE(I): Kinetic energy of the ith atom

PLANE: Alpha-numeric array for lattice orientation

POT: Potential energy between two atoms

PPE(I): Potential energy of the ith atom

PPTC: Primary potential function evaluated at ROE

PTE(I): Total energy of the ith atom (potential + kinetic)

PTMAS: Target mass in kilograms

RE: Input Morse potential parameter

RLL: Reciprocal of LL

RO: Spacing constant in FCC(110) lattice generation subroutine

ROE: Nearest neighbor distance

ROE2: ROE squared

ROEA: Maximum cut off for Born-Mayer potential

ROEB: Minimum cut off for Morse potential

ROEC: Maximum cut off for Morse potential

ROEC2: ROEC squared

ROEL: Radius inside of which local potential energy is found

ROEL2: ROEL squared

ROEM: ROE-DTI, region in which modification of repulsive force
must be made

RX(I), RY(I), RZ(I): x,y,z coordinates of an ith atom at any time

RXI(I), RYI(I), RZI(I): x,y,z coordinates of an ith atom's initial
position

RXK(I), RYK(I), RZK(I): x,y,z coordinates of temporary position of
an ith atom during force cycle

SAVE: $\frac{1}{2}$ POT

SCX, SCY, SCZ: x,y,z coordinate scale factors

START: An optional timing variable, not used in this simulation

SUM: Variable in cubic fit subroutine

TARGET: Alpha-numeric array for target material

TSAVE: Bullet mass/(target mass + bullet mass); distributes potential energy between target and bullet

TE: Total energy of all crystal atoms (kinetic + potential)

TEMP: Temperature of lattice in degrees Kelvin. Not used in this simulation

TEFAC: Product of DTI * CVD

TFAC: A time factor ratio used to determine DT by maximum force method

TFACB: TFAC for the bullet

THERM: Thermal energy of atom. Not used in this simulation

TIME: Elapsed problem time in seconds

TLPE: Total local potential energy of atoms within a radius ROEL

TLPEØ: TLPE at time zero

TMAS: Target atom mass in amu

TPKE: Total kinetic energy of all crystal atoms

TPOT: Total potential energy of all crystal atoms

TPOTL: Storage position for the last computed value TPOT

VSS: Storage variable for velocity components

VX(I), VY(I), VZ(I): x,y,z components of ith atoms velocity

X, Y, Z: Unscaled coordinates used in crystal generation

XSTART: X Coordinate used in impact point generator

YLAX(I): Relaxation in -y direction of ith layer in L.U.

ZP: Floating point form of JTT

COMPUTER PROGRAM

THE FOLLOWING PROGRAM IS THE ONE USED FOR THE STATIC SIMULATION RUNS. THE DYNAMIC PROGRAM IS ESSENTIALLY THE SAME AS THE STATIC. IN THE DYNAMIC PROGRAM, SUBROUTINES (B100) AND (PLACE) ARE OMITTED, AND THE INITIAL ATOM POSITIONS ARE READ IN ON DATA CARDS. ALSO, AN IMPACT POINT GENERATOR PACKAGE IS INCLUDED IN THE DYNAMIC PROGRAM. BOTH PROGRAMS CALCULATE THE EQUATIONS OF MOTION FOR THE SYSTEM THROUGH THE USE OF THE APPROPRIATE POTENTIAL FUNCTION AND THE AVERAGE FORCE METHOD OF INTEGRATION. THE NET DISTANCE OF MOVEMENT, VELOCITY, AND ENERGY VALUES ARE PRINTED OUT FOR THE DESIRED ATOMS ON SELECTED TIMESTEP NUMBERS. THE FINAL POSITION, VELOCITY, AND ENERGY VALUES FOR EACH ATOM ARE SUMMARIZED AT THE END OF THE PROGRAM.

// EXEC FORTHCLG, TIME.GO=20, REGION.GO=140K

// FORT.SYSIN DD *

C

DIMENSION VX(1000), VY(1000), VZ(1000), PKE(1000)

DIMENSIONING OF VARIABLES NOT NEEDED IN COMMON

C

DIMENSION DX(1000), DY(1000), DZ(1000), PTE(1000)

DIMENSION RXK(1000), RYK(1000), RZK(1000)

COMMON LABELING OF VARIABLES REQUIRED IN OTHER SUBROUTINES

COMMON/COM1/RX(1000), RY(1000), RZ(1000), LCUT(1000),

1LL, LD, ITYPE, NVAC

COMMON/COM2/IH1(20), IH2(8), IHS(10), IHB(6), IHT(6),

1TARGET(4), TMAS, BULLET(4), BMAS, PLANE, TEMP, THERM

COMMON/COM3/RXI(1000), RYI(1000), RZI(1000), CVR, EVR,

1NT, TIME, DT, DTI, ILAY

1IVACX, IVACY, IVACZ

COMMON/COM4/IX, IY, IZ, SCX, SCY, SCZ, IDEEP, D1X, D1Y, D1Z,

COMMON/COM5/ROE, ROE2, ROEM, EXA, EXB, PEXA, PEXB, FXA, PFXA,

1IQ, TSAVE, BSAVE

COMMON/COM6/FX(1000), FY(1000), FZ(1000), PAC, PEPTC, FM

COMMON/COM7/PPTC, TPOT, PPE(1000), TLPE, ROEL, ROEL2, NEW

COMMON/COM8/ROEA, ROEB, ROEC, ROEC2, CP0, CP1, CP2, CP3,

1CFO, CF1, CF2, CGD1, CGD2, CGB1, CGB2, CGF1, CGF2

COMMON/COMA/ A(4,5), MCRO

C

READ STATEMENT FORMATS

9010 FORMAT(20A4)

9020 FORMAT(8A4, 3F8.5, 2F5.2)

9030 FORMAT(4A4, 3F8.5, 6A4, F6.2)

9040 FORMAT(F6.3, 5X, I5, 6I4, 3F5, 3I2)

9050 FORMAT(10A4, A4, 4I3, F8.4, I4, F5.3)

C

WRITE STATEMENT FORMATS

9610 FORMAT(1H1)

9620 FORMAT(47X, 'SUMMARY OF ATOMS' //, 35X, 8A4, ' ', NT = 'I4, //, 13(' ATOM POSITION BIND ENERGY ' '), //)

9630 FORMAT(3(I5, 3F6.2, F8.4, 8X))

9640 FORMAT(/4X, F10.3, 25H EV, TOTAL KINETIC ENERGY, , F10.3, 1H EV, TOTAL POTENTIAL ENERGY, F10.3, ' EV, REDUCTION', 1//60X 'RADIUS = ', F5.2,)

9650 FORMAT(105X, 4HPAGE, I3, /, 1H1)

9660 FORMAT(/ ' ATOM DX DY PE DZ TE' /) 1VX VY VZ KE

9670 FORMAT(1I8, 3F10.3, 3F10.1, 3F10.4)

9680 FORMAT(' SHARP DT DECREASE ', 2E10.3)

9690 FORMAT(I4, 3F5.2, I4)

9691 FORMAT(9F8.4)

9692 FORMAT(1X, I4, /)

C

INITIALIZING

START=0.01*ITIME(XX)

DO 2 I=1, 1000

RXK(I)=0.0

RYK(I)=0.0

RZK(I)=0.0

VX(I)=0.0


```

VY(I)=0.0
VZ(I)=0.0
PKE(I)=0.0
PPE(I)=0.0
PTE(I)=0.0
2 RZI(I)=0.0
ISHUT=1
NRUN=0

```

C

INPUT DATA

```

READ ( 5,9010) IH1
READ ( 5,9020) IH2,DCON,ALPHA,RE,ROEC,ROEL
READ ( 5,9030) BULLET,BMAS,PEXA,PEXB,IHB,THERM
READ ( 5,9030) TARGET,TMAS,EXA,EXB,IHT,TEMP
READ ( 5,9050) IHS,PLANE,LS,IX,IY,IZ,CVR,MCRO ,DTI

```

C

CONSTANTS AND SCALING FACTORS

```

DTIS=DTI
ROE2=4.0
ROE=SQRT(ROE2)
ROEM = ROE-DTI
ROEL2=ROEL*ROEL
CVE=1.60E-19
CVM=1.672E-27
VFAC=.50
FM=1.0E-10
FM2=FM*FM
CVD=CVR*1.0E-10
CVED=CVE/CVD
PTMAS=TMAS*CVM
PBMAS=BMAS*CVM
HTMAS=0.5*PTMAS/CVE
HBMAS=0.5*PBMAS/CVE
TSAVE=BMAS/(BMAS+TMAS)
BSAVE=TMAS/(BMAS+TMAS)

```

C

REPULSIVE POTENTIAL PARAMETERS

```

FXA=ALOG(-EXB*CVED)+EXA
PFXA=ALOG(-PEXB*CVED)+PEXA
PPTC=EXP(PEXA+PEXB*ROE)
PAC=ALOG(CVED)+PEXA
PFPTC=EXP(PAC+PEXB*ROE)

```

C

ATTRACTIVE POTENTIAL PARAMETERS

```

CGD1=ALOG(DCON)+2.0*ALPHA*RE
CGD2=ALOG(2.0*DCON)+ALPHA*RE
CGB1=-2.0*ALPHA*CVR
CGB2=-ALPHA*CVR
CGF1=ALOG(-CGB1*CVED)+CGD1
CGF2=ALOG(-CGB2*CVED)+CGD2

```

C

CUTOFF DISTANCES FOR ATTRACTIVE AND REPULSIVE POTENTIALS

```

ROEA=1.50/CVR
ROEB=2.0/CVR
ROEC2=ROEC*ROEC

```

C

PARAMETERS FOR CALCULATION OF THE BEST CUBIC FIT IN THE GAP BETWEEN MAXIMUM DISTANCE CUTOFF OF THE REPULSIVE POTENTIAL (ROEA), AND MINIMUM DISTANCE CUTOFF OF THE ATTRACTIVE POTENTIAL (ROEB). SUBROUTINE CROSYM ACTUALLY PERFORMS THIS CURVE FITTING.

```

A(1,1)=1.0
A(1,2)=ROEA
A(1,3)=ROEA*ROEA
A(1,4)=ROEA**3
A(1,5)=EXP(EXA+EXB*ROEA)
A(2,1)=1.0

```



```

A(2,2)=ROEB
A(2,3)=ROEB*ROEB
A(2,4)=ROEB**3
A(2,5)=EXP(CGD1+CGB1*ROEB)-EXP(CGD2+CGB2*ROEB)
A(3,1)=0.0
A(3,2)=-1.0
A(3,3)=-2.0*ROEA
A(3,4)=-3.0*ROEA*ROEA
A(3,5)=EXP(FXA+EXB*ROEA)/CVED
A(4,1)=0.0
A(4,2)=-1.0
A(4,3)=-2.0*ROEB
A(4,4)=-3.0*ROEB*ROEB
A(4,5)=(EXP(CGF1+CGB1*ROEB)-EXP(CGF2+CGB2*ROEB))/CVED
CALL CROSYM
CP0=A(1,5)
CP1=A(2,5)
CP2=A(3,5)
CP3=A(4,5)
CF0=-CP1*CVED
CF1=-2.0*CP2*CVED
CF2=-3.0*CP3*CVED
5 READ ( 5,9040) EVR,NTT,NS,ND,IP,IDEEP,ITYPE,NVAC,D1X,
1 D1Y,D1Z,IVACX,IVACY,IVACZ
IF(NTT.EQ.0) GO TO 9999
IQ=ITYPE-1
EV=EVR*1.0E+3

```

SELECTION OF THE DESIRED CRYSTAL STRUCTURE AND ORIENTATION. 100, 110, AND 111 PLANES OF FACE-CENTERED, BODY-CENTERED, AND DIAMOND STRUCTURES ARE ALLOWED. ILAY AND IDEEP ARE VARIABLES ESTABLISHING THE NUMBER OF MOBILE LAYERS IN THE CRYSTAL. RXI(I) AND PYI(I) ARE VARIABLES SAVING THE ORIGINAL X-POSITION OF THE I' TH ATOM. Y AND Z POSITIONS ARE ANALOGOUS.

```

14 CALL B100
30 ILAY=IDEEP
IF(IDEEP) 35,35,40
35 LD=LL
ILAY=IY
40 RLL=1.0/LL
TPOTL=1.0
DO 45 I=1,LL
RXK(I)=RX(I)
RYK(I)=RY(I)
RZK(I)=RZ(I)
RXI(I)=RX(I)
RYI(I)=RY(I)
45 RZI(I)=RZ(I)

```

C
THIS SECTION ALLOWS ONE TO REPEAT A RUN OF THE PROGRAM WITH DIFFERENT DATA WITHOUT REPEATING INITIALIZATION, POTENTIAL PARAMETER CALCULATIONS AND CRYSTAL LATTICE BUILDING. SUBROUTINE PLACE USES LCUT(I) AND NVAC TO CREATE VACANCIES, INTERSTITIALS, AND REPLACEMENT IMPURITIES AT DESIRED LOCATIONS IN THE LATTICE.

```

IF(NRUN.EQ.0) GO TO 60
DO 55 I=1,LL
LCUT(I)=0
RX(I)=RXI(I)
RY(I)=RYI(I)
RZ(I)=RZI(I)
RXK(I)=RXI(I)
RYK(I)=RYI(I)
55 RZK(I)=RZI(I)
60 NRUN=1
CALL PLACE
RXI(1)=RX(1)
RYI(1)=RY(1)
RZI(1)=RZ(1)

```



```

RXK(1)=RX(1)
RYK(1)=RY(1)
RZK(1)=RZ(1)
DO 65 I=1,LL
VX(I)=0.0
VY(I)=0.0
VZ(I)=0.0
PPE(I)=0.0
PKE(I)=0.0
65 PTE(I)=0.0
TPOT=0.0
NEW=0

```

C
THE ENERGY SUBROUTINE CALCULATES THE POTENTIAL ENERGY OF EACH ATOM IN THE LATTICE. SUBROUTINE LOCAL SUMS UP THIS ENERGY FOR ALL ATOMS WITHIN A SPECIFIC RADIUS OF THE POINT DEFECT. THIS SECTION PRINTS OUT X, Y, AND Z COORDINATES, IN LATTICE UNITS, AND BINDING ENERGIES OF EACH ATOM IN THE CRYSTAL AT TIME ZERO.

```

CALL ENERGY
BIND=-TPOT
TE=TPOT+BIND

```

C
TIME=0.0
NT=0
WRITE (6,9610)
WRITE (6,9620) IH2,NT
DO 70 I=1,LL,3
K=I+1
J=I+2
70 WRITE (6,9630) I,RX(I),RY(I),RZ(I),PPE(I),K,RX(K),
1RY(K),RZ(K),PPE(K),J,RX(J),RY(J),RZ(J),PPE(J)
WRITE (6,9640) TPKE,TPOT,TE,ROEL
NPAGE=1
NPAGE=NPAGE+1
WRITE (6,9650) NPAGE

C
THIS IS THE MAIN BODY OF THE PROGRAM. BY USE OF THE AVERAGE FORCE METHOD, EXPLAINED IN REF. 13, IT DOES ALL THE DYNAMICS FOR EACH INDIVIDUAL ATOM. SUBROUTINE STEP CALCULATES ALL MUTUAL FORCES AMONG THE ATOMS. BASED ON THE FORCES, THIS SECTION THEN CALCULATES TEMPORARY POSITIONS FOR THE PRIMARY, AND ALL OTHER ATOMS; RECALCULATES FORCES IN STEP; AND THEN RECALCULATES FINAL POSITIONS FOR THE PRIMARY AND ALL OTHER ATOMS, BASED ON THE AVERAGE OF THESE TWO FORCES. THIS SECTION ALSO INCLUDES ALL KINETIC ENERGY CALCULATIONS, BASED ON THE VELOCITIES INVOLVED; AND FINALLY CALCULATES A NEW TIMESTEP DURATION FOR USE IN THE NEXT TIME-STEP, BASED ON EITHER A MAXIMUM ALLOWED FORCE, OR MAXIMUM ALLOWED ENERGY. VELOCITIES ARE HALVED AT THE END OF EACH TIMESTEP AS A METHOD OF DAMPING.

```

DT=1.0E-15
DDTI=.005
NDEC=0
100 DTI=DTI-DDTI
NDEC=NDEC+1
DTOD=DT/CVD
TFAC=2.0*PTMAS*DTI*CVD
TFACB=2.0*PBMAS*DTI*CVD
TEFAC=DTI*CVD
HDTOD=0.5*DTOD
DTOM=DT/PTMAS
HDTOM=0.5*DTOM
DTOMB=DT/PBMAS
HDTOMB=0.5*DTOMB
200 CALL STEP
IF(LCUT(1).GT.0) GO TO 240
I=1
RXK(I)=RX(I)

```



```

    RYK(I)=RY(I)
    RZK(I)=RZ(I)
    RX(I)=RX(I)+DTOD*(HDTOMB*FX(I)+VX(I))
    RY(I)=RY(I)+DTOD*(HDTOMB*FY(I)+VY(I))
    RZ(I)=RZ(I)+DTOD*(HDTOMB*FZ(I)+VZ(I))
240 DO 245 I=2,LD
    IF(LCUT(I).GT.0)GO TO 245
    RXK(I)=RX(I)
    RYK(I)=RY(I)
    RZK(I)=RZ(I)
    RX(I)=RX(I)+DTOD*(HDTOM*FX(I)+VX(I))
    RY(I)=RY(I)+DTOD*(HDTOM*FY(I)+VY(I))
    RZ(I)=RZ(I)+DTOD*(HDTOM*FZ(I)+VZ(I))
245 CONTINUE
    CALL STEP
    EMAX=0.0
    FMAX=0.0
    TIME=TIME+DT
    NT=NT+1
    IF(LCUT(1).GT.0) GO TO 265
    I=1
    VSS=VX(I)
    VX(I)=VSS+HDTOMB*FX(I)
    RX(I)=RXK(I)+(VX(I)+VSS)*HDTOD
    VSS=VY(I)
    VY(I)=VSS+HDTOMB*FY(I)
    RY(I)=RYK(I)+(VY(I)+VSS)*HDTOD
    VSS=VZ(I)
    VZ(I)=VSS+HDTOMB*FZ(I)
    RZ(I)=RZK(I)+(VZ(I)+VSS)*HDTOD
    PKE(I)=VX(I)*VX(I)+VY(I)*VY(I)+VZ(I)*VZ(I)
    EMAX1=PKE(I)
    FMAX1=FX(I)*FX(I)+FY(I)*FY(I)+FZ(I)*FZ(I)
    DTE1=TEFAC*SQRT(1.0/FMAX1)
    DTF1=SQRT(TFACB/FMAX1)
260 FX(I)=0.0
    FY(I)=0.0
    FZ(I)=0.0
265 DO 280 I=2,LD
    IF(LCUT(I).GT.0)GO TO 280
    VSS=VX(I)
    VX(I)=VSS+HDTOM*FX(I)
    RX(I)=RXK(I)+(VX(I)+VSS)*HDTOD
    VSS=VY(I)
    VY(I)=VSS+HDTOM*FY(I)
    RY(I)=RYK(I)+(VY(I)+VSS)*HDTOD
    VSS=VZ(I)
    VZ(I)=VSS+HDTOM*FZ(I)
    RZ(I)=RZK(I)+(VZ(I)+VSS)*HDTOD
    PKE(I)=VX(I)*VX(I)+VY(I)*VY(I)+VZ(I)*VZ(I)
275 F2=FX(I)*FX(I)+FY(I)*FY(I)+FZ(I)*FZ(I)
    FX(I)=0.0
    FY(I)=0.0
    FZ(I)=0.0
    IF(F2.GT.FMAX) FMAX=F2
    IF(PKE(I).GT.EMAX) EMAX=PKE(I)
280 CONTINUE
    DTL=DT
    CTIME=0.01*ITIME(XX)-START
    DTE=TEFAC*SQRT(1.0/EMAX)
    DTF=SQRT(TFAC/FMAX)
    IF(EMAX1.GT.EMAX) EMAX=EMAX1
    DT=DTE1
    IF(DT.GT.DTF1) DT=DTF1
    IF(DT.GT.DTE) DT=DTE
    IF(DT.GT.DTF) DT=DTF
    IF(DT.GT.1.0E-14) DT=1.0E-14
300 IF(ISHUT.EQ.-1) GO TO 400
310 IF(NS-NT) 400,400,320
320 DO 325 I=1,LL
    VX(I)=VFAC*VX(I)
    VY(I)=VFAC*VY(I)

```



```

325 VZ(I)=VFAC*VZ(I)
GO TO 800

```

C THE PRINT SUBROUTINE PLACES A HEADING OF PERTINENT INFORMATION AT THE TOP OF EACH TIMESTEP PRINTOUT. POTENTIAL ENERGY AND LOCAL POTENTIAL ENERGY FOR EACH ATOM ARE CALCULATED BASED ON THE NEW POSITIONS. SUMMATIONS OF TOTAL POTENTIAL AND KINETIC ENERGY FOR THE LATTICE ARE PERFORMED. DX, DY, AND DZ KEEP TRACK OF MOTION RELATIVE TO THE INITIAL POSITION AT TIME ZERO FOR EACH ATOM.

```

400 CALL PRINT
C
410 TPOT=0.0
DO 450 I=1,LL
PPE(I)=0.0
450 PTE(I)=0.0
CALL ENERGY
PKE(I)=HBMAS*PKE(I)
TPKE=TPKE+PKE(I)
PTE(I)=PKE(I)+PPE(I)
DO 620 I=2,LL
PKE(I)=HTMAS*PKE(I)
TPKE=TPKE+PKE(I)
620 PTE(I)=PKE(I)+PPE(I)
TE=TPOT+BIND
WRITE ( 6,9660)
DTEST=(RY(1)-RYI(1))**2
IF (DTEST.GT. 0.01) DTEST= 0.01
IF(TPOT.LE.TPOTL) GO TO 700
ERAT=TPKE*RLL
700 DO 750 I=1,LD
DX(I)=RX(I)-RXI(I)
DY(I)=RY(I)-RYI(I)
DZ(I)=RZ(I)-RZI(I)
IF (DX(I)**2.GE.DTEST) GO TO 720
IF (DY(I)**2.GE.DTEST) GO TO 720
IF (DZ(I)**2.GE.DTEST) GO TO 720
GO TO 750

```

C THIS SECTION PRINTS THE RELATIVE MOTION, VELOCITY, AND ENERGY OF EACH ATOM, FOR EVERY TIMESTEP SO DESIGNATED: IE, EVERY ND*TH TIMESTEP, BEGINNING WITH #NS AND ENDING WITH #NTT.

```

720 WRITE ( 6,9670) I,DX(I),DY(I),DZ(I),VX(I),VY(I),
1VZ(I),PKE(I),PPE(I),PTE(I)
750 CONTINUE
WRITE ( 6,9640) TPKE,TPOT,TE,ROEL
WRITE ( 6,9650) NPAGE
NPAGE=NPAGE+1
TPOTL=TPOT
IF(NT-NTT) 760,950,950
760 DO 780 I=1,LL
VX(I)=VFAC*VX(I)
VY(I)=VFAC*VY(I)
VZ(I)=VFAC*VZ(I)
780 CONTINUE
IF(ISHUT.EQ.-1) GO TO 950
790 NS=NS+ND
800 IF (NDEC.EQ.10) GO TO 810
GO TO 100
810 DDTI=0.1*DDTI
DTI=DTI+DDTI
NDEC=0
GO TO 100
950 CONTINUE

```

C THIS SECTION PRINTS OUT X, Y, AND Z COORDINATES AND BINDING ENERGIES OF EACH ATOM IN THE CRYSTAL AT THE END OF THE PROGRAM. ALSO, DATA CARDS ARE PRINTED WITH X,Y,Z COORDINATE OF EACH ATOM IN THE CRYSTAL FOR USE IN THE DYNAMIC PROGRAM.


```

955  WRITE ( 6,9620) IH2,NT
      WRITE (7,9690) LL,D1X,D1Y,D1Z,NVAC
      DO 965 I=1,LL,3
      K=I+1
      J=I+2
      WRITE (7,9691) RX(I),RY(I),RZ(I),RX(K),RY(K),RZ(K),RX
1RZ(J)
965  WRITE ( 6,9630) I,RX(I),RY(I),RZ(I),PPE(I),K,RX(K),
1RY(K),RZ(K),PPE(K),J,RX(J),RY(J),RZ(J),PPE(J)
      WRITE ( 6,9640) TPKE,TPOT,TE,ROEL
      WRITE ( 6,9650) NPAGE
1000 IF(ISHUT) 9999,5,5
9999 STOP
      END

```

SUBROUTINE CROSYM

C SOLVES M SIMULTANEOUS EQUATIONS BY THE METHOD OF CROUT
THIS SUBROUTINE FITS THE BEST CUBIC BETWEEN THE REPULSIVE
AND ATTRACTIVE PARTS OF THE POTENTIAL.

C

```

COMMON/COMA/ A(4,5),MCRO
M=MCRO
N=M+1
I1=1
100  I3=I1
      SUM=ABS(A(I1,I1))
      DO 120 I=I1,M
      IF(SUM-ABS(A(I,I1))) 110,120,120
110  I3=I
      SUM=ABS(A(I,I1))
120  CONTINUE
      IF(I3-I1) 130,150,130
130  DO 140 J=1,N
      SUM=-A(I1,J)
      A(I1,J)=A(I3,J)
140  A(I3,J)=SUM
150  I3=I1+1
      DO 160 I=I3,M
160  A(I,I1)=A(I,I1)/A(I1,I1)
170  J2=I1-1
      I3=I1+1
      IF(J2) 180,200,180
180  DO 190 J=I3,N
      DO 190 I=1,J2
190  A(I1,J)=A(I1,J)-A(I1,I)*A(I,J)
      IF(I1-M) 200,220,200
200  J2=I1
      I1=I1+1
      DO 210 I=I1,M
      DO 210 J=1,J2
210  A(I,I1)=A(I,I1)-A(I,J)*A(J,I1)
      IF(I1-M) 100,170,100
220  DO 240 I=1,M
      J2=M-I
      I3=J2+1
      A(I3,N)=A(I3,N)/A(I3,I3)
      IF(J2) 230,250,230
230  DO 240 J=1,J2
240  A(J,N)=A(J,N)-A(I3,N)*A(J,I3)
250  RETURN
      END

```

C

SUBROUTINE B100
 THIS IS A LATTICE GENERATOR THE THE BCC (100) ORIENTATION.
 THE CRYSTAL IS DEVELOPED IN THE ORDER, X FOLLOWED BY Z,
 FOLLOWED BY Y.
 IT CONTAINS A NONSTANDARD USE OF THE SURFACE RELAXATION
 PARAMETER.

C

```

COMMON/COM1/RX(1000),RY(1000),RZ(1000),LCUT(1000),
1LL,LD,ITYPE,NVAC
COMMON/COM4/IX,IY,IZ,SCX,SCY,SCZ,IDEEP,D1X,D1Y,D1Z,
1IVACX,IVACY,IVACZ
DIMENSION YLAX(20)
DATA YLAX/20*0.0/
YLAX(1)=-0.20
YLAX(2)=-0.03
SCX=1.0
SCY=1.0
SCZ=1.0
M = 2
JT=0
Y=-SCY
DO 60 J=1,IY
Y=Y+SCY
KT=0
Z=-SCZ
DO 59 K=1,IZ
Z=Z+SCZ
IT=0
X=-SCX
DO 58 I=1,IX
X=X+SCX
IF(IT-(IT/2)*2) 21,11,21
11 IF(JT-(JT/2)*2) 57,12,57
12 IF(KT-(KT/2)*2) 57,30,57
21 IF(JT-(JT/2)*2) 22,57,22
22 IF(KT-(KT/2)*2) 30,57,30
30 RX(M)=X
RY(M)=Y+YLAX(J)
RZ(M)=Z
M=M+1
IF (IT.NE.IVACX) GO TO 57
IF (JT.NE.IVACY) GO TO 57
IF (KT.NE.IVACZ) GO TO 57
NVAC=M-1
57 IT=IT+1
58 CONTINUE
KT=KT+1
59 CONTINUE
JT = JT + 1
IF(IDEEP-JT) 60,110,60
60 CONTINUE
LL=M-1
100 RETURN
110 LD=M-1
GO TO 60
END
```

SUBROUTINE PLACE

C

THIS SUBROUTINE LOCATES A VACANCY, INTERSTITIAL, OR REPLACEMENT IMPURITY IN THE LATTICE.

C

```

COMMON/COM1/RX(1000),RY(1000),RZ(1000),LCUT(1000),
1LL,LD,ITYPE,NVAC
COMMON/COM4/IX,IY,IZ,SCX,SCY,SCZ,IDEEP,D1X,D1Y,D1Z,
1IVACX,IVACY,IVACZ
GO TO (10,20,30,40), ITYPE
```



```

10 LCUT(NVAC) = 1
   LCUT(1) = 1
   RX(1)=0.0
   RY(1)=0.0
   RZ(1)=0.0
   GO TO 50
20 RX(1)=RX(NVAC)+D1X
   RY(1)=RY(NVAC)+D1Y
   RZ(1) = RZ(NVAC) + D1Z
   GO TO 50
30 LCUT(NVAC) = 1
   RX(1) = RX(NVAC)
   RY(1) = RY(NVAC)
   RZ(1) = RZ(NVAC)
   GO TO 50
40 RX(1)=RX(NVAC)+D1X
   RY(1)=RY(NVAC)+D1Y
   RZ(1) = RZ(NVAC)+D1Z
50 RETURN
   END

```

SUBROUTINE STEP

C
THIS SUBROUTINE DOES THE DYNAMICS FOR ONE TIMESTEP.
THE FIRST HALF DOES THE DYNAMICS FOR ATOM #1; THE SECOND
HALF FOR ALL OTHERS.

```

C
COMMON/COM1/RX(1000),RY(1000),RZ(1000),LCUT(1000),
1LL,LD,ITYPE,NVAC
COMMON/COM5/ROE,ROE2,ROEM,EXA,EXB,PEXA,PEXB,FXA,PFXA,
1IQ,TSAVE,BSAVE
COMMON/COM6/FX(1000),FY(1000),FZ(1000),PAC,PFPTC,FM
COMMON/COM8/ROEA,ROEB,ROEC,ROEC2,CPO,CP1,CP2,CP3,
1CF0,CF1,CF2,CGO1,CGO2,CGB1,CGB2,CGF1,CGF2
IF (IQ-1) 100,101,102
100 IP=2
   GO TO 200
101 IP=1
   GO TO 200
102 I=1
   IP=2
105 DO 195 J=IP,LL
   IF(LCUT(J)) 195,110,195
110 DRX=RX(J)-RX(I)
   IF(DRX) 113,117,117
113 IF(DRX+ROE) 195,195,120
117 IF(DRX-ROE) 120,195,195
120 DRY=RY(J)-RY(I)
   IF(DRY) 123,127,127
123 IF(DRY+ROE) 195,195,130
127 IF(DRY-ROE) 130,195,195
130 DRZ=RZ(J)-RZ(I)
   IF(DRZ) 133,137,137
133 IF(DRZ+ROE) 195,195,140
137 IF(DRZ-ROE) 140,195,195
140 DIST=DRX*DRX+DRY*DRY+DRZ*DRZ
   IF(DIST-ROE2) 150,195,195
150 DIST=SQRT(DIST)
160 IF(DIST-ROEM) 162,162,165
162 FORCE=EXP(PFXA+PEXB*DIST)
   GO TO 180
165 DFF=ROE-DIST
   IF(DFF-1.0E-10) 195,195,167
167 FORCE=(EXP(PAC+PEXB*DIST)-PFPTC)/DFF
180 IF(FM-FORCE) 190,190,195
190 FOD=FORCE/DIST
   FA=FOD*DRX
   FX(J)=FX(J)+FA
   FX(I)=FX(I)-FA
   FA=FOD*DRY
   FY(J)=FY(J)+FA

```



```

        FY(I)=FY(I)-FA
        FA=FOD*DRZ
        FZ(J)=FZ(J)+FA
        FZ(I)=FZ(I)-FA
195  CONTINUE
C
200  DO 300 I=IP,LD
      IF(LCUT(I)) 300,205,300
205  IP=I+1
      DO 295 J=IP,LL
        IF(LCUT(J)) 295,210,295
210  DRX=RX(J)-RX(I)
        IF(DRX) 213,217,217
213  IF(DRX+ROEC) 295,295,220
217  IF(DRX-ROEC) 220,295,295
220  DRY=RY(J)-RY(I)
        IF(DRY) 223,227,227
223  IF(DRY+ROEC) 295,295,230
227  IF(DRY-ROEC) 230,295,295
230  DRZ=RZ(J)-RZ(I)
        IF(DRZ) 233,237,237
233  IF(DRZ+ROEC) 295,295,240
237  IF(DRZ-ROEC) 240,295,295
240  DIST=DRX*DRX+DRY*DRY+DRZ*DRZ
        IF(DIST-ROEC2) 250,295,295
250  DIST=SQRT(DIST)
        IF(DIST-ROEA) 260,255,255
255  IF(DIST-ROEB) 265,270,270
260  FORCE=EXP(FXA+EXB*DIST)
        GO TO 280
265  FORCE=DIST*(DIST*CF2+CF1)+CF0
        GO TO 280
270  FORCE=EXP(CGF1+CGB1*DIST)-EXP(CGF2+CGB2*DIST)
280  IF(ABS(FORCE).LE.FM) GO TO 295
        FOD = FORCE/DIST
        FA=FOD*DRX
        FX(J)=FX(J)+FA
        FX(I)=FX(I)-FA
        FA=FOD*DRY
        FY(J)=FY(J)+FA
        FY(I)=FY(I)-FA
        FA=FOD*DRZ
        FZ(J)=FZ(J)+FA
        FZ(I)=FZ(I)-FA
295  CONTINUE
300  CONTINUE
      RETURN
      END

```

SUBROUTINE ENERGY

C THIS SUBROUTINE CALCULATES THE MUTUAL POTENTIAL ENERGIES.
 THE FIRST HALF DOES THE DYNAMICS FOR ATOM #1; THE SECOND
 HALF FOR ALL OTHERS.

```

C
  COMMON/COM1/RX(1000),RY(1000),RZ(1000),LCUT(1000),
1LL,LD,ITYPE,NVAC
  COMMON/COM5/ROE,ROE2,ROEM,EXA,EXB,PEXA,PEXB,FXA,PFXA,
1IQ,TSAVE,BSAVE
  COMMON/COM7/PPTC,TPOT,PPE(1000),TLPE,ROEL,ROEL2,NEW
  COMMON/COM8/ROEA,ROEB,ROEC,ROEC2,CP0,CP1,CP2,CP3,
1CF0,CF1,CF2,CGD1,CGD2,CGB1,CGB2,CGF1,CGF2
  IF (IQ-1) 100,101,102
100 IP=2
    GO TO 200
101 IP=1
    GO TO 200
102 I=1
    IP=2
105 DO 595 J=IP,LL
      IF(LCUT(J)) 595,510,595

```



```

510 DRX=RX(J)-RX(I)
    IF(DRX) 513,517,517
513 IF(DRX+ROE) 595,595,520
517 IF(DRX-ROE) 520,595,595
520 DRY=RY(J)-RY(I)
    IF(DRY) 523,527,527
523 IF(DRY+ROE) 595,595,530
527 IF(DRY-ROE) 530,595,595
530 DRZ=RZ(J)-RZ(I)
    IF(DRZ) 533,537,537
533 IF(DRZ+ROE) 595,595,540
537 IF(DRZ-ROE) 540,595,595
540 DIST=DRX*DRX+DRY*DRY+DRZ*DRZ
    IF(DIST-ROE2) 550,595,595
550 DIST=SQRT(DIST)
560 POT=EXP(PEXA+PEXB*DIST)-PPTC
580 TPOT=TPOT+POT
    PPE(I)=PPE(I)+BSAVE*POT
    PPE(J)=PPE(J)+TSAVE*POT
595 CONTINUE
600 CONTINUE

```

C

```

200 DO 300 I=IP,LD
    IF(LCUT(I)) 300,205,300
205 IP=I+1
    DO 295 J=IP,LL
        IF(LCUT(J)) 295,210,295
210 DRX=RX(J)-RX(I)
    IF(DRX) 213,217,217
213 IF(DRX+ROEC) 295,295,220
217 IF(DRX-ROEC) 220,295,295
220 DRY=RY(J)-RY(I)
    IF(DRY) 223,227,227
223 IF(DRY+ROEC) 295,295,230
227 IF(DRY-ROEC) 230,295,295
230 DRZ=RZ(J)-RZ(I)
    IF(DRZ) 233,237,237
233 IF(DRZ+ROEC) 295,295,240
237 IF(DRZ-ROEC) 240,295,295
240 DIST=DRX*DRX+DRY*DRY+DRZ*DRZ
    IF(DIST-ROEC2) 250,295,295
250 DIST=SQRT(DIST)
    IF(DIST-ROEA) 260,255,255
255 IF(DIST-ROEB) 265,270,270
260 POT=EXP(EXA+EXB*DIST)
    GO TO 280
265 POT=DIST*(DIST*(DIST*CP3+CP2)+CP1)+CPO
    GO TO 280
270 POT=EXP(CGD1+CGB1*DIST)-EXP(CGD2+CGB2*DIST)
280 TPOT=TPOT+POT
    SAVE=0.5*POT
    PPE(I)=PPE(I)+SAVE
    PPE(J)=PPE(J)+SAVE
295 CONTINUE
300 CONTINUE
    RETURN
END

```

SUBROUTINE PRINT

C

THIS SUBROUTINE PRINTS THE HEADING OF ALL PERTINENT INFORMATION AT THE TOP OF EACH TIMESTEP PRINTOUT.

C

```

COMMON/COM1/RX(1000),RY(1000),RZ(1000),LCUT(1000),
1LL,LD,ITYPE,NVAC
COMMON/COM2/IH1(20),IH2(8),IHS(10),IHB(6),IHT(6),
1TARGET(4),TMAS,BULLET(4),BMAS,PLANE,TEMP,THERM
COMMON/COM3/RXI(1000),RYI(1000),RZI(1000),CVR,EVR,
1NT,TIME,DT,DTI,ILAY
COMMON/COM4/IX,IY,IZ,SCX,SCY,SCZ,IDEEP,D1X,D1Y,D1Z,
1IVACX,IVACY,IVACZ

```



```

COMMON/COM5/ROE,ROF2,ROEM,EXA,EXB,PEXA,PEXB,FXA,PFXA,
1IQ,TSAVE,BSAVE
COMMON/COM8/ROFA,ROEB,ROEC,ROEC2,CPO,CP1,CP2,CP3,
1CF0,CF1,CF2,CGD1,CGD2,CGB1,CGB2,CGF1,CGF2
9710 FORMAT(40X,10A4,/,28X,20A4,/)
9720 FORMAT(9H TARGET -,4A4,10HPRIMARY -,4A4,1X,14HLATTICE
1 UNIT =,F7.4,4H ANG)
9730 FORMAT(4X,6HMASS =,F7.2,13X,6HMASS =,F7.2,9X,14HLATTIC
1E TEMP =F5.2,7H DEG K,,18H THERMAL CUTOFF =,F5.2,3H E
1V/)
9740 FORMAT(2H (,A4,8H) PLANE,,18H PRIMARY ENERGY =,
1 F5.2,21HKEV, CRYSTAL SIZE (,I2,3H X ,I2,3H X',I2,3H
1 ),,4X,16HVACANCY IN SITE ,I4/)
9741 FORMAT(2H (,A4,8H) PLANE,,18H PRIMARY ENERGY =,
1 F5.3,21HKEV, CRYSTAL SIZE (,I2,3H X ,I2,3H X',I2,3
1H ),,4X,INTERSTITIAL (' ,2(F5.2,' ,'),F5.2,' ) FROM
1SITE ',I4/)
9742 FORMAT(2H (,A4,8H) PLANE,,18H PRIMARY ENERGY =,
1 F5.2,21HKEV, CRYSTAL SIZE (,I2,3H X ,I2,3H X',I2,3H
1 ),,4X,20HREPLACEMENT IN SITE ,I4/)
9750 FORMAT(30H PRIMARY START POINT (LU) X =,F5.2,5H, Y =,
1F5.2,5H, Z =,F5.2,5X,I3,' LAYERS ARE FREE TO MOVE',
110X,4HIQ =,I2/)
9760 FORMAT(12H POTENTIAL ,6A4,3X,5HPEXA=,F9.5,2X,5HPEXB=,
1F9.5,2X,5HPFXA=,F9.5)
9765 FORMAT(12X,6A4,3X,5HEXA =,F9.5,2X,5HEXB =,F9.5,2X,5HFX
1A =,F9.5/)
9770 FORMAT(' WHEN',F8.4,' < R <',F8.4,' THE MATCHING POTEN
1TIAL PARAMETERS ARE',/,,' CPO =',F10.3,', CP1 =',
1F10.3,', CP2 =',F10.3,', CP3 =',F10.3,/,,' CF0 =',
1E10.3,', CF1 =',E10.3,', CF2 =',E10.3,/)
9780 FORMAT(' CUT-OFF AT',F5.2,', WHEN R > ',F6.3,' LU, MOR
1SE POTENTIAL PARAMETERS ARE',8A4,/,,' 10X,' CGD1 =',
1F8.4,', CGD2 =',F8.4,', CGB1 =',F8.4,', CGB2 =',F8.4,
1', CGF1 =',F8.4,', CGF2 =',F8.4,/)
9790 FORMAT(10H TIMESTEP ,I4,22X,6HDTI = , F5.4, 5H LU,
1,22H ELAPSED TIME (SEC) =, E10.4,', NEXT TIMESTEP IS
1=,E10.4/)
WRITE ( 6,9710) IHS,IH1
WRITE ( 6,9720) TARGET,BULLET,CVR
WRITE ( 6,9730) TMAS,BMAS,TEMP,THERM
GO TO (401,402,403,402), ITYPE
401 WRITE ( 6,9740) PLANE,EVR,IX,IY,IZ,NVAC
GO TO 405
402 WRITE ( 6,9741) PLANE,EVR,IX,IY,IZ,D1X,D1Y,D1Z,NVAC
GO TO 405
403 WRITE ( 6,9742) PLANE,EVR,IX,IY,IZ,NVAC
405 WRITE ( 6,9750) RXI(1),RYI(1),RZI(1),ILAY,IQ
WRITE ( 6,9760) IHB,PEXA,PEXB,PFXA
WRITE ( 6,9765) IHT,EXA,EXB,FXA
WRITE ( 6,9770) ROEA,ROEB,CPO,CP1,CP2,CP3,CF0,CF1,CF2
WRITE ( 6,9780) ROEC,ROEB,IH2,CGD1,CGD2,CGB1,CGB2,
1CGF1,CGF2
WRITE ( 6,9790) NT,DTI,TIME,DT
RETURN
END

```

```

BLOCK DATA
DIMENSIONING OF VARIABLES USED IN COMMON
COMMON/COM1/RX(1000),RY(1000),RZ(1000),LCUT(1000),
1LL,LD,ITYPE,NVAC
DATA RX/1000*0.0/,RY/1000*0.0/,RZ/1000*0.0/,LCUT/1000*
COMMON/COM3/RXI(1000),RYI(1000),RZI(1000),CVR,EVR,
1INT,TIME,DT,DTI,ILAY
DATA RXI/1000*0.0/,RYI/1000*0.0/,RZI/1000*0.0/
COMMON/COM6/FX(1000),FY(1000),FZ(1000),PAC,PFPTC,FM
DATA FX/1000*0.0/,FY/1000*0.0/,FZ/1000*0.0/
END
//GO.FT06F001 DD SPACE=(CYL,(10,2),RLSE)
//GO.SYSIN DD *
CRYSTAL-1968 MODIFIED TO DEAL WITH VACANCIES AND INTERSTITI

```


(GIRIFALCO--WEIZER POTENTIAL)				.99060	1.41160	3.03200	3.4
ARGON	39.948	9.33	-5.60	ARGON-TUNGSTEN			
TUNGSTEN	183.86	11.30	-7.50	TUNGSTEN-TUNGSTEN			
BODY CENTERED CUBIC, (100) ORIENTATION				100	10	10	10
	100	5	4	51	0.7	-0.7	0.0 5 1

BIBLIOGRAPHY

1. Gay, W.L., Harrison, D.E., Jr., "Machine Simulation of Collisions Between a Copper Atom and a Copper Lattice," The Physical Review, v. 135, No. 6A, p. A1780-A1790, 14 Sept 1964.
2. Harrison, D.E., Jr., Levy, N.S., Johnson, J.P. III, and Effron, H.M., "Computer Simulation of Sputtering," Journal of Applied Physics, v. 39, No. 8, p. 3742-3761, July 1968.
3. Harrison, D.E., Jr., "Additional Information on Computer Simulation of Sputtering," Journal of Applied Physics, v. 40, No. 9, p. 3870-3872, August 1969.
4. Harrison, D.E., Jr., Greiling, D.S., "Computer Studies of Xenon-Ion Ranges in a Finite-Temperature Tungsten Lattice," Journal of Applied Physics, v. 38, No. 8, p. 3200-3211, July 1967.
5. Gibson, J.B., Goland, A.N., Milgram, M. and Vineyard, G.H., "Dynamics of Radiation Damage," The Physical Review, v. 120, No. 4, p. 1229-1253, November 15, 1960.
6. Johnson, R.A., Brown, E., "Point Defects in Copper," The Physical Review, v. 127, No. 2, p. 446-454, 15 July 1962.
7. Erginsoy, C., Vineyard, G.H., and Englert, A., "Dynamics of Radiation Damage in a Body-Centered Cubic Lattice," The Physical Review, v. 133, No. 2A, p. A595-A606, 20 January 1964.
8. Kornelsen, E.V., Sinha, M.K., "Thermal Release of Inert Gases from a (100) Tungsten Surface," Journal of Applied Physics, v. 39, No. 10, p. 4546-4555, September 1968.
9. Kornelsen, E.V., Sinha, M.K., "Thermal Release of Inert Gases from Tungsten; Dependence on the Crystal Face Bombarded," paper presented at Conference on Atomic Collision and Penetration Studies Using Energetic Ions, Chalk River, September 1967.
10. Johnson, R.A., "Point Defect Calculations for an fcc Lattice," The Physical Review, v. 145, No. 2, p. 423-433, 13 May 1966.
11. Johnson, R.A., "Point-Defect Calculations in Alpha Iron," American Society for Metals, Chap. 27, p. 357-370, 1965.
12. Harrison, D.E., Jr., Leeds, R.W., and Gay, W.L., "Computer Studies of Copper Atom Ranges in Copper Lattices," v. 36, No. 10, p. 3154-3161, October 1965.

13. Harrison, D.E., Jr., Gay, W.L., and Effron, H.M., "Algorithm for the Calculation of the Classical Equations of Motion of an N-Body System," Journal of Mathematical Physics, v. 10, No. 7, July 1969.
14. Vine, G.L., Computer Simulation of Copper and Tungsten Crystal Dynamics With Vacancies and Interstitials, M.S. Thesis, Naval Postgraduate School, Monterey, California 1971.
15. Levy, N.D., Computer Simulation of the Sputtering Process, M.S. Thesis, Naval Postgraduate School, Monterey, California, 1965.
16. Johnson, J.P., Calculation of Surface Binding Energies by Computer Simulation of the Sputtering Process, M.S. Thesis, Naval Postgraduate School, Monterey, California, 1966.
17. Effron, H.M., Correlation of Argon-Copper Sputtering Mechanisms With Experimental Data Using a Digital Computer Simulation Technique, M.S. Thesis, Naval Postgraduate School, Monterey, California 1967.
18. Moore, W.L., Digital Computer Simulation of Xenon Ions Channeling in the (100) Tungsten Channel at Various Lattice Temperatures, M.S. Thesis, Naval Postgraduate School, Monterey, California 1969.
19. Harrison, D.E., Jr., unpublished research.
20. Girifalco, L.A., Wizer, V.G., "Application of the Morse Potential Function to Cubic Metals," The Physical Review, v. 114, No. 3, p. 687-690, 1 May 1959.

INITIAL DISTRIBUTION LIST

	No. Copies
1. Defense Documentation Center Cameron Station Alexandria, Virginia 22314	2
2. Library, Code 0212 Naval Postgraduate School Monterey, California 93940	2
3. Professor D.E. Harrison, Jr. Department of Physics, Code 61Hx Naval Postgraduate School Monterey, California 93940	3
4. Captain James A. Tankovich C/O Mr. Delbert H. Bays Box 74 Gatesville, North Carolina 27938	1

Unclassified

Security Classification

DOCUMENT CONTROL DATA - R & D

(Security classification of title, body of abstract and indexing annotation must be entered when the overall report is classified)

ORIGINATING ACTIVITY (Corporate author)

Naval Postgraduate School
Monterey, California 93940

2a. REPORT SECURITY CLASSIFICATION

Unclassified

2b. GROUP

REPORT TITLE

Computer Simulation of Split Interstitial Equilibrium Positions and Binding
Energies in a Tungsten Crystal

DESCRIPTIVE NOTES (Type of report and inclusive dates)

Master's Thesis, June 1972

AUTHOR(S) (First name, middle initial, last name)

James Anthony Tankovich

REPORT DATE

June 1972

7a. TOTAL NO. OF PAGES

69

7b. NO. OF REFS

20

CONTRACT OR GRANT NO.

PROJECT NO.

9a. ORIGINATOR'S REPORT NUMBER(S)

9b. OTHER REPORT NO(S) (Any other numbers that may be assigned
this report)

DISTRIBUTION STATEMENT

Approved for public release; distribution unlimited.

SUPPLEMENTARY NOTES

12. SPONSORING MILITARY ACTIVITY

Naval Postgraduate School
Monterey, California 93940

ABSTRACT

Computer simulations were performed to locate the equilibrium positions and binding energies of interstitial He, Ne, Ar, Kr, and Xe in a tungsten crystal. Heavy interstitial atoms in tungsten share a lattice site with the atom that normally occupies that site and form what is called a split interstitial. Three characteristic interstitial sites were located relative to each lattice site tested. The distance of the impurity atom from the site was seen to vary roughly inversely with its mass, and the displacement of the lattice atom increased with the mass of the impurity atom.

The foreign atom in its interstitial position was tested to determine the minimum initial kinetic energy needed to escape the lattice, as well as the optimum escape direction. The minimum energy may be interpreted to be the binding energy of the defect. A comparison of experimental binding energies from Kornelsen and Sinha and simulated binding energies indicates the model gives realistic results.

4.

KEY WORDS

LINK A

LINK B

LINK C

ROLE

WT

	ROLE
1.	Chairman
2.	Vice Chairman
3.	Secretary
4.	Treasurer
5.	Member
6.	Member
7.	Member
8.	Member
9.	Member
10.	Member
11.	Member
12.	Member
13.	Member
14.	Member
15.	Member
16.	Member
17.	Member
18.	Member
19.	Member
20.	Member
21.	Member
22.	Member
23.	Member
24.	Member
25.	Member
26.	Member
27.	Member
28.	Member
29.	Member
30.	Member
31.	Member
32.	Member
33.	Member
34.	Member
35.	Member
36.	Member
37.	Member
38.	Member
39.	Member
40.	Member
41.	Member
42.	Member
43.	Member
44.	Member
45.	Member
46.	Member
47.	Member
48.	Member
49.	Member
50.	Member
51.	Member
52.	Member
53.	Member
54.	Member
55.	Member
56.	Member
57.	Member
58.	Member
59.	Member
60.	Member
61.	Member
62.	Member
63.	Member
64.	Member
65.	Member
66.	Member
67.	Member
68.	Member
69.	Member
70.	Member
71.	Member
72.	Member
73.	Member
74.	Member
75.	Member
76.	Member
77.	Member
78.	Member
79.	Member
80.	Member
81.	Member
82.	Member
83.	Member
84.	Member
85.	Member
86.	Member
87.	Member
88.	Member
89.	Member
90.	Member
91.	Member
92.	Member
93.	Member
94.	Member
95.	Member
96.	Member
97.	Member
98.	Member
99.	Member
100.	Member

WT

ROLE

WT

Defect binding energy

Thesis
T1365
c.1

Tankovich

134807

Computer simulation of
split interstitial
equilibrium positions
and binding energies in
a tungsten crystal.

Thesis
T1365
c.1

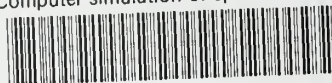
Tankovich

134807

Computer simulation of
split interstitial
equilibrium positions
and binding energies in
a tungsten crystal.

thesT1365

Computer simulation of split interstitia



3 2768 002 05452 0

DUDLEY KNOX LIBRARY